TARGETED DRUG-LOADED NANOPARTICLE SYSTEM (TDNPS) TO AMELIORATE AND TREAT IDIOPATHIC LUNG FIBROSIS

By

HARISH RAMACHANDRAMOORTHY

DISSERTATION

Submitted in fulfillment of the requirements

for the degree of Doctor of Philosophy at

The University of Texas at Arlington

December 2022

Arlington, Texas

Dissertation Supervisor

Dr. Kytai T. Nguyen

Professor of Bioengineering

Supervising Committee

Dr. Yong Yang, Associate Professor of Biomedical Engineering at University of North Texas

Dr. Liping Tang, Professor of Bioengineering

Dr. Debabrata Saha, Associate Professor of Radiation Oncology at UT Southwestern

Dr. Hao Xu, Assistant Professor of Bioengineering

Abstract

Idiopathic pulmonary fibrosis (IPF) is a fatal progressive disease with a dismal prognosis and 3-5 years of survival. Up to date, there are no effective treatments, and a few current therapies that do not ameliorate the pulmonary fibrosis but rather just increase the survival time by 2-3 years. The major factor limiting the treatment is the lack of targeted therapies to deliver the drugs past the mucosa, into the disease microenvironment. To combat this disease, we proposed a localized therapy via our targeted drug-loaded nanoparticles (TDNPs) to effectively deliver drugs and treat lung fibrosis. Our objective was to design TDNPs that should pass the thick mucus layer and release potent drugs at the lung fibrosis tissue in a controlled manner. Our designed TDNPs are comprised of an FDA approved drug Pirfenidone that inhibits the pro-fibrotic cytokines. Furthermore, the TDNP is tagged with antibodies against Fibroblast Activation Protein (FAP), which is overexpressed in the diseased tissue so that the targeting and retention of the nanoparticle at the fibrosis site could be enhanced. We also developed a novel lung fibrosis-on-chip platform to evaluate the effectiveness of the TDNP modality with highest precision surpassing the drawbacks of conventional therapeutic efficiency testing. Three specific aims followed are: 1) To design and characterize TDNPs for treating lung fibrosis, 2) To determine the therapeutic efficiency of TDNPs through 2-D and 3-D based *in vitro* studies, and 3) To evaluate the therapeutic effectiveness of our designed NPs using lung fibrosis animal models. The TDNPs were successfully fabricated with a size <500nm that was optimal for deep alveolar delivery. The NPs had sustained release of drugs up to 3 days and high stability for the same time period. We also demonstrated that the NPs, due to their PEGylated surface, were able to penetrate the mucus layer and the collagen matrix layer that mimic the *in vivo* conditions significantly higher than that of the PLGA NPs. TDNPs showed more than a 2-fold increase in uptake and accumulation in fibrotic

cells significantly higher than that of non-targeted NPs showing the effectiveness of FAP targeting. The NPs also displayed significantly higher therapeutic efficiency by reducing the expression level of αSMA by around 5 & 7-fold in 2D and 3D fibrosis models, respectively compared to that of the free drug. The TDNPs were also able to localize and retain significantly more in the lung tissue compared to the PLGA NPs. We have thus showed that the synthesized TDNPs would serve as a functional drug delivery system that can pass the pulmonary barriers and deliver drugs to the injured lung tissue to treat pulmonary fibrosis.

Acknowledgements

I would like to acknowledge and dedicate my thesis to my family for supporting and helping me through my Ph.D. journey, without whom this would not be possible. I would also like to extend my warmest thanks and greatest gratitude to my mentor Dr. Kytai Nguyen, who has been no less than a mother to me, guiding and encouraging me throughout my Ph.D. degree. She has helped me grow as an independent researcher who can run and manage a laboratory. During the whole COVID-19 pandemic, she went above and beyond to make sure all the students in the lab were safe. I would also like to extend a special shout out to Dr. Serkan Yaman, for training, mentoring me and supporting me as a brother.

I sincerely thank all my collaborators and committee members: to Dr. Yong Yang for his support and guidance with my thesis project, to Dr. Debabrata Saha for his guidance and help with my experiments, to Dr. Liping Tang for taking his valuable time in reviewing my thesis and helping me with my animal studies, to Dr. Hao Xu for his valuable time to review my work and give his best advice to improve my research, and to Dr. Jon A. Weidanz for his advice and guidance in various projects throughout my thesis work.

I would like to extend my gratitude to the Department of Bioengineering and its staff for their continued support and funding through my Ph.D.

I also would like to take this opportunity to thank Priyanka Iyer, Dr. Uday Chintapula, Dr. Tam Nguyen, Luis Soto, Aneetta Kuriakose, and Tanviben Kotadia for their friendship and support throughout my journey. I would like to extend my thanks to all the Ph.D. students of Dr. Nguyen's lab for their help and support. Lastly, I extend my thanks and appreciation to my friends, who have stood by my side and supported me as a family throughout my Ph.D. journey.

December 14th, 2022

Table of Contents

List of Figures

Chapter 1

LITERATURE REVIEW

1.1 Ideopathic Pulmonary Fibrosis (IPFs)

Idiopathic pulmonary fibrosis (IPF) is a chronic, progressive life-threatening disease with an unknown origin and limited therapeutic options. IPF affects almost 3 million people worldwide and around 100,000 people in the US alone (**Figure 1**)[1, 2]. It has an estimated median survival of 2-5 years[3-6]. It has a stiff collagenous extracellular matrix (ECM) and is a complex disease that involves with impaired cellular signaling from multiple cell types such as fibroblasts, epithelial, endothelial, and immune cells, uncontrolled migration and proliferation of various cells, including fibroblasts, scarring of the lung parenchyma, and irreversible loss of lung functions[7]. The rate of collagen production in the lung interstitium exceeds the rate of collagen digestion, and thus, the interstitial layer starts becoming rigid as the excess collagen accumulates in the ECM matrix. This in turn prevents gas exchange through the endothelium[8] (**Figure 2**). Unfortunately, there is no cure for lung fibrosis, and the only viable option is lung transplantation[9]; yet the portion of patients who die while waiting for transplantation ranges up to 67%.

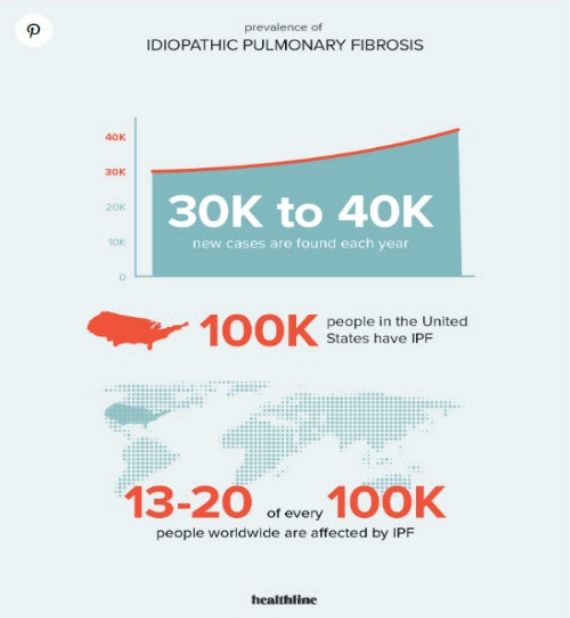

Figure 1. ***The prevalence of IPF in the US.*** *Sources on November, 2022.* https://www.healthline.com/health/managing-idiopathic-pulmonary-fibrosis/ipf-facts#prevalence

1.2 Current treatment of IPFs and their limitations

1.2.1 Nonpharmacological treatments for IPF

Currently lung transplantation is the only viable nonpharmacological treatment for IPF[10, 11]. Though transplantation does not guarantee a permanent cure for IPF, it is more advantageous as it improves the survival time and reduces symptoms[12]. There should also be consideration of the possible side effects caused from lung transplantation including cardiac dysfunction, diabetes and organ rejection[13].

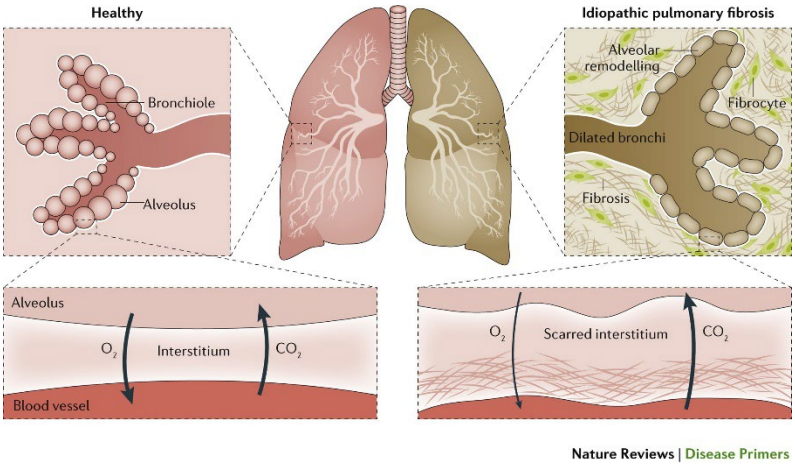

Figure 2. Effects of IPF on the lung tissue. The alveolar remodeling due to scar tissue causes excess collagen secretion and stiffness in the interstitial layer, in turn reducing gas exchange through the endothelium.
Martinez, F., Collard, H., Pardo, A. et al. Idiopathic pulmonary fibrosis. *Nat Rev Dis Primers* 3, 2017, 17074.

The patient would be undergoing either unilateral or bilateral lung transplantation based on their condition and urgency; unilateral transplantation has a shorter wait time and less post-transplantation complications. On the other hand, bilateral transplantations have better pulmonary function after transplantation[14]. Though transplantation prolongs the survival rate of the patients, their overall 5-year post-transplantation survival rate is still less than 50%[15].

1.2.2 Pharmacological treatments for IPF

Currently, there are just two FDA approved drugs to treat IPF, namely Pirfenidone and Nintedanib, which have shown to reduce the rate of disease progression and increase the lung functions in clinical trials of IPF patients[16, 17]. Pirfenidone is a modified pyridine small molecule that has anti-fibrotic and anti-inflammatory properties. Clinical trials showed that Pirfenidone was

able to reduce both rates of fibrosis by suppressing TGFβ cytokine and of collagen production[18, 19]. Pirfenidone, however, has been shown to cause abnormal liver function in some patients where there were elevated levels of serum alanine aminotransferase and bilirubin production[7, 20, 21].

Nintedanib, on the other hand, is an intracellular tyrosine kinase inhibitor, which binds to the adenosine triphosphate binding sites, thereby interferring with the signaling pathways of vascular endothelial growth factor (VEGF), platelet-derived growth factor (PDFG), and fibroblast growth factor (FGF) receptors[22]. Though Nintedanib showed improved lung functions and reduced severe side effects in clinical trial IPF patients, the death rate remained the same[23]. The drug also showed severe hepatotoxicity in a few patients.

Recently, in a preclinical study, TD139, a novel inhibitor targeting Galectin-3 was tested in a Bleomycin induced mouse model. The study showed an elevated expression of Galectin-3 in a Bleomycin induced fibrosis model and that inhibiting the protein attenuated lung fibrosis[24]. The drug is currently in phase 2 clinical trials. Ziritaxestat (GLPG1690), a potent autotaxin inhibitor, is also in clinical trials for IPF treatment. The drug showed effective reduction in Lysophosphatidic Acid levels *in vivo* and also showed higher inhibition of Autotaxin compared to that of FDA approved drugs[25].

Though various drugs are being developed to improve lung functions, reduce scarring and revert back fibrotic conditions, they still face two main obstacles: 1) the delivered drug does not reach the lung interstitium because of scarring, mucus and exhalation, and 2) the systemic toxicity of these drugs is very severe. To overcome these limitations, novel drug carriers are being focused to deliver the drugs to the interstitium past the barriers[26].

1.3 Nanoparticles for IPF treatment

Nanotechnology has recently gained attention as effective drug delivery systems for numerous diseases due to their varied advantages including increased bioavailability, reduced side effects, and ease of surface modification[27]. The wide variety of nano-formulations and ease of controlling the drug pharmacokinetics and pharmacodynamics attract many researchers investigating in the nanomedicine field. In chronic lung diseases including fibrosis, nanotechnology based drug carriers act as the key to overcoming the many obstacles of intratracheal delivery[28]. Nanoparticles can be tuned in size to deliver the drugs at the specified disease region (upper/lower respiratory track). They also help avoid expulsion of the drugs and enzymatic degradation of the payload. It has also been shown that nanoparticles with a size ranging from 1-1000 nm can get the payload deeper into the alveoli[29].

Though there are various types of nanoparticles, nanoparticles made from synthetic polymers including poly(lactic-co-glycolic acid) (PLGA), poly(ε-caprolactone) (PCL), poly(lactic acid) (PLA), polystyrene (PS), and poly(ethylene glycol) (PEG) are studied extensively for pulmonary drug delivery[30, 31]. Of those, PLGA nanoparticles show to be the ideal system among the other polymers, due to their unique properties including that they 1) are biodegradable and biocompatible, 2) can load a broad spectrum of drugs and proteins, 3) are easy to modify/conjugate molecules onto the nanoparticle surface, and 4) size can be controlled with ease. For instance, Ruchit et al. showed enhanced delivery of Pirfenidone to the fibrotic tissue and a higher therapeutic efficiency of IPF in Bleomycin induced fibrosis model[32]. Thus, PLGA polymers would be an ideal candidate for payload delivery in pulmonary fibrosis.

1.4 PEGylation strategies for mucus penetration

Though the nanoparticles provide resistance from drug degradation, sustained release of the payloads in the lung interstitium and reduced cytotoxic effect, it is still prone to mucus adhesion and rapid clearance even before reaching the lung epithelium. To overcome this issue, researchers have turned their attention to mucus penetrating nanoparticles[33].

Perhaps the most pioneered research is from the Hanes's group in understanding the mechanism of mucus penetration by studying viruses travelling through mucus; its results showed that the neutral charge of the viral surface and lack of hydrophobic surface regions resulted in reduced mucus interactions[34]. PEG has also been the most studied polymer due to its hydrophilic nature and neutral charge[35]. NPs used for diseases with a mucus barrier have been conjugated or physically coated with PEG to give them a muco-inert surface, in turn aiding in the mucus penetrating properties[36].

PEG conjugated/coated polystyrene have long been studied for their muco-inert properties. PS-PEG NPs with size >200 nm was shown to have effective resistance against mucoadhesion and enhanced mucus penetration in airways mucus collected from lung fibrosis[37, 38]. PLGA-PEG has recently been focused on as mucus penetrating NPs due to their biocompatibility and ability to carry both hydrophilic and hydrophobic drugs[39]. It was shown that coating nanoparticles with a dense PEG layer shielded them from adhesive interactions with mucus constituents aiding to their rapid penetration through low-viscosity fluid between mucin fibers[40, 41]. Interestingly, studies also showed that NPs coated with 2-5 KDa PEG showed higher muco-penetrating properties compared to that of PEG $\geq$ 10 KDa[42].

1.5 Targeting strategies for IPF

Though delivering drugs to the disease microenvironment significantly increases therapeutic efficiency compared to systemic administration of drugs, targeted therapies always stay a step ahead. To understand the effective targeting moiety to use, we first have to understand the key player of the disease. In IPF, myofibroblasts have been the focus as the factor that controls and regulates fibrosis[43]. Myofibroblasts are responsible for excess ECM secretion resulting in the scarring of lung tissues. Targeting these myofibroblasts and reverting them back to quiescent fibroblasts would effectively reverse fibrosis. However, the challenge lies in finding a target that is expressed specifically in the fibrotic cells.

Fibroblast activation protein-α (FAP) is a type II integral serine protease, which has been shown to overexpress in patients with IPF. It is observed that FAP has very minimal to no expression on healthy lung tissues, but has been shown to overexpress in lung tissue remodeling[44]. Suraj et al. showed the effectiveness of FAP as a myofibroblast target[45]. They showed the enhanced therapeutic effects of FAP-targeted PI3Ki on a Bleomycin induced fibrosis model compared to the non-targeted control. They showed that FAP targeting enhanced the targeting and retention of the drug in fibrotic tissue and produced significantly higher therapeutic efficiency than the control. An intensive meta-analysis of a huge group of IPF patients conducted by Penghui et al showed the high expression and dependence of FAP protein in the disease progression of IPF[46]. Therefore, using an FAP targeting antibody to selectively target the myofibroblast and deliver the drugs would enhance the therapeutic efficiency while eliminating systemic toxicity.

1.6 Models for assessment of IPF treatments

Though many drugs and drug carrier systems show excellent results in laboratory conditions, they fail to show similar results in the pre-clinical and clinical studies. This is especially true in the case of pulmonary lung fibrosis[47]. There is a need for more advanced *in vitro* models that replicate the disease microenvironment mimicking an *in vivo* model before going into clinical trials. This also helps provide a patient specific testing to verify if the drug works for each individual patient. Thus 2.5D and 3D models have been areas of great focus as they can overcome the limitations of conventional 2D *in vitro* models. A few of the major advantages of 2.5D and 3D models are listed in **Figure 3**.

2D	2.5D and 3D
migration, chemotaxis and traction in X and Y planes	migration, chemotaxis and traction in X,Y and Z planes
high stiffness	low and tunable stiffness to match in vivo tissues
forced apical-basal polarity	no forced polarity
cellular adhesions in X and Y plane	cellular adhesions in X, Y and Z plane
fewer cell-cell and cell-matrix interactions	greater cell-cell and cell-matrix interactions
no soluble gradients	presence of soluble gradients
air-liquid interface (ALI) epithelial maturation not possible	supports air-liquid interface (ALI) epithelial maturation

Figure 3. Advantages of 2.5D and 3D *in vitro* cultures over conventional 2D *in vitro* cultures.
Sundarakrishnan A, Engineered cell and tissue models of pulmonary fibrosis. *Adv Drug Deliv Rev*. 2018 Apr;129:78-94.

Transwell systems have been widely used as 2.5D models to study the airway epithelial cells in Air-liquid interface (ALI)-induced epithelial maturation, which is the first step for any injury model[48]. Prasad et al. used the co-culture transwell system to study the reduction in migration of IPF cells due to the impaired paracrine epithelial PDGF signaling[49]. Studies have shown that the complex 3D structures produced by airway epithelial and microvascular endothelial cells on 2.5D Matrigel is not reproducible by 2D systems[50-52]. Huang et al. showed that the effect of anti-angiogenic peptide kallistatin on reducing VEGF and VEGFR2 expression in the 2.5D Matrigel assay was much more comparable to the *in vivo* model[53]. Though the 2.5D system shows great

advantage over the conventional system, it still faces some limitations including lack of mechanical tunability and multi layered cellular interactions.

When focusing on the key players in fibrosis (fibroblasts), a much more complex testing system is required. Hydrogel based systems, especially made from collagen type 1, is highly preferred for fibroblast culture as it closely mimics the *in vivo* ECM condition[54]. Acid-solubilized animal collagen I undergoes de novo fibrillogenesis at neutral pH[55]. Fibroblasts added during polymerization encapsulate, attach and contract the collagen hydrogel network via integrin adhesions[54]. Arora et al showed that the degree of collagen gel compliance was directly proportional to α-SMA expression level by studying the fibroblast-mediated collagen contraction[56]. This correlation plays a very important role in designing the experiment[57, 58]. We will be utilizing the 3D collagen based model to test the effectiveness of the nanoparticle and to design the 3D organ on chip, which would take us closer to the clinical model.

1.7.1 Overview of dissertation research

To overcome the current limitations, our long-term goal for this research is to develop and investigate the effectiveness of novel site-specific targeted drug-loaded nanoparticles (TDNPs) that can penetrate the mucus barrier and deliver the anti-fibrotic/anti-inflammation drug to reduce/reverse fibrosis process while consisting of minimal off-target severe side effects.

1.7.2 Specific aims

Aim 1: Formulating and characterizing TDNPs that are made from biodegradable and biocompatible PLGA-PEG copolymer, loaded with FDA approved Pirfenidone, and used for targeting myofibroblasts via FAP antibodies. The synthesized NPs were characterized for their

physicochemical properties like size, charge, and stability. The drug release kinetics for therapeutic application were analyzed. Finally, their mucus penetrating effect was analyzed to consider if they were an ideal drug carrier system for intratracheal delivery.

Aim 2: Determining the *in vitro* efficiency of the formulated TDNPs. The NPs were analyzed for their effectiveness in targeting activated myofibroblasts through *in vitro* uptake studies. The therapeutic efficiency of these NPs was analyzed *in vitro* to access the effectiveness of these NPs to prevent myofibroblast transition. The cytocompatibility of TDNPs was also analyzed in healthy lung cells including epithelial and fibroblast cells. 2.5D fibrosis models were created to act as a transition bridge between laboratory and clinical models. The NPs were tested for their therapeutic efficiency in the 2.5D fibrosis model.

Aim 3: Evaluating the *in vivo* effectiveness of the TDNPs in Bleomycin induced IPF model. The targeting and retention efficiency of the NPs on lung tissues of the mice were tested using Rhodamine B loaded TDNPs. The therapeutic efficiency of TDNPs was evaluated by analyzing the reduction in scarring and lung structure after treatment. Masson's trichrome staining analysis was also performed to analyze the reduction in collagen deposition after treatment with TDNPs.

1.7.3 Innovative aspects

The innovative aspect of this thesis research is that firstly, we created a novel biodegradable nanoparticle system that not only can penetrate the lung mucosa, but can also target the myofibroblasts for a more enhanced delivery of payload in the fibrotic microenvironment. This nanoparticle system further serves as a drug carrier for both hydrophilic and hydrophobic drugs for pulmonary drug delivery. Our modified 3D fibrotic model will help transition the model into a fully functional organ-on-chip fibrosis model.

Chapter 2

MATERIALS AND METHODS

2.1 Materials used

All chemicals, if not specified, were purchased from Sigma-Aldrich (St. Louis, MO). PLGA-PEG and PLGA-PEG-NHS (Molecular weight 17kDa - 5kDa) was purchased from Akina Inc. (West Lafayette, IN); Rhodamine B dye was purchased from Sigma-Aldrich (St. Louis, MO). Iscove's Modified Dulbecco's Medium (IMDM), Fetal bovine serum, penicillin-streptomycin, and trypsin-ethylenediaminetetraacetic acid (EDTA) were procured from Fischer Scientific (Waltham, MA).

2.2.1 Formulation of DNPs

The drug loaded PLGA-PEG nanoparticles are synthesized using a modified version of the standard single emulsion (oil/water) technique (**Figure 4**). Briefly, 20 mg of Pirfenidone is added to 50 mg (5:1) w/w of PLGA-PEG: PLGA-PEG-(N-Hydroxysuccinimide), and the mixture is dissolved in 2 ml of DCM (oil phase). After the polymers are completely dissolved, the solution is added dropwise to 5 ml of 2% Polyvinyl alcohol (PVA) solution (water phase) under constant stirring and sonicated for 1 minute at 20W for emulsification. The solution is then added dropwise to 15 ml of 2% Polyvinyl alcohol (PVA) solution under constant stirring at room temperature and then sonicated at 25W for 2 minutes. The solvent is evaporated by overnight stirring at room temperature. The particles are collected by centrifugation at 22,00 RPM for 25 minutes at 10°C. The supernatant was used to measure the drug loading efficiency via an indirect method. The pellet is washed twice and resuspended in 3 mL DI water with 5% mannitol mixture. The particles were freeze-dried for 24 hours. Blank NPs were prepared by the same process mentioned above without adding the Pirfenidone in the oil phase.

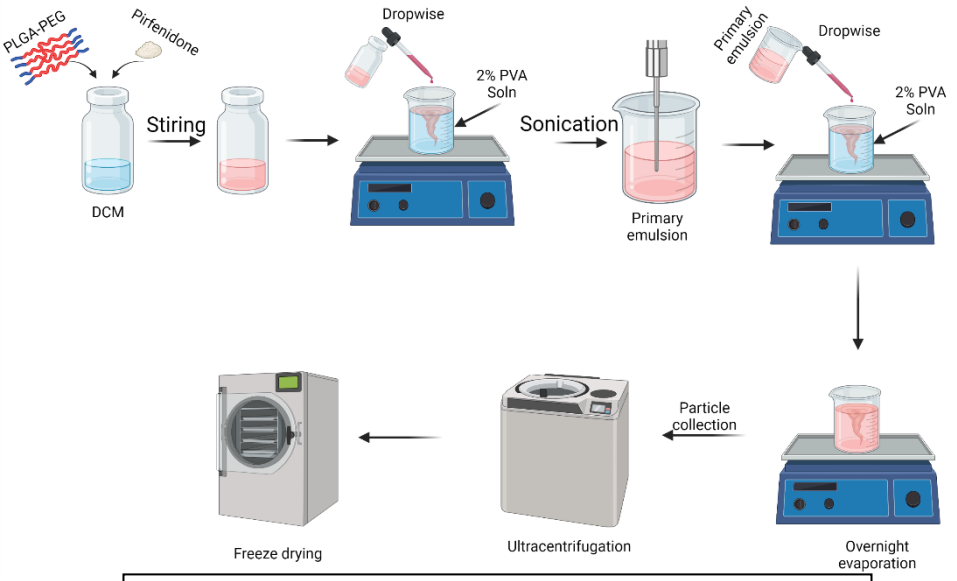

Figure 4. Schematic of DNP synthesis

2.2.2 Formulation of TDNPs

To synthesize FAP antibody conjugated nanoparticles (TDNPs), simple NHS based conjugation previously optimized from our group was used. Briefly, 10 mg of drug-loaded NPs is taken at 2 mg/ml concentration (MES buffer) and 10 µg of FAP antibody per mg of nanoparticles will be added to the suspension under stirring at 4°C for 2 hours. TDNPs will be then collected by centrifugation and freeze-drying. Depending on whether the application is towards human IPF or mouse IPF cells, respective antibodies would be used (human target - R & D Systems cat -AF3715, mouse target - R & D Systems cat -MAB9727).

2.2.1 Physicochemical properties of TDNPs

The physicochemical characteristics of TDNPs including size, charge and polydispersity index was measured using NanoBrook 90Plus PALS analyzer (Brookhaven Instruments, Holtsville, NY). For DLS measurements, 50 µL of 1 mg/mL NP suspension is added to a transparent cuvette containing 3 mL of DI water and the size measurement was performed using a

perpendicular laser. Zeta potential (charge) measurements were done using a probe attachment placed inside the cuvette.

The surface morphology of the formulated nanoparticles was visualized by transmission electron microscopy (TEM). Briefly, freeze-dried nanoparticle samples in DI water were fixed onto ozone treated copper grids and stained with uranyl acetate (0.5%). A H-7500 TEM (Hitachi) transmission electron microscope was used to visualize the particle morphologies.

Freeze-dried material including PLGA-PEG polymer, PLGA polymer, and PEG were analyzed using Fourier-Transform infrared spectroscopy (FTIR). Briefly, FTIR spectra of the varied materials were recorded in transmission mode using FT-IR Nicolet-6700 in the range of 400 to 4000cm^{-1}.

2.2.2 Drug loading of TDNPs

Drug loading efficiency of the nanoparticles will be determined by direct loading using a UV-Vis spectrophotometer. Briefly, 2 mg of TDNP were measured in a glass vial. 2 mL of chloroform was added to break the nanoparticles. The solvent was evaporated and 1 mL of ethanol was added to dissolve the Pirfenidone. The solution was centrifuged at 10,000 RPM for 10 minutes and the supernatant was analyzed at 313 nm using a UV-Vis spectrophotometer.

$$Drug\ loading\ efficiency\ ((\%)\ ) = \frac{Total\ drug\ in\ NP}{Initial\ drug\ used}\ x\ 100\% \qquad (1)$$

2.2.3 Drug release kinetics of TDNPs

To analyze the drug release kinetics of TDNPs, 8 mg of TDNPs were dispersed in 2 ml of PBS 7.4 pH. The solution was then split equally into 4 tubes and incubated at 37°C. At designated times (0 hours, 2 hours, 6 hours, 12 hours, 1 day, 2 days, 3 days, 5 days), each sample was centrifuged at 17,000 RPM for 20 minutes to collect the supernatant, the NPs were then re-

suspended in fresh PBS solution and incubated at 37°C until the next time point. The supernatants were characterized for the drug amount using UV-Vis spectrophotometer at 313 nm.

2.2.4 TDNP stability

Stability of the TDNPs were determined by analyzing their change in size over a period of 72 hours in human simulated lung fluid[59]. Briefly, TDNPs and blank NPs were dispersed and incubated in simulated lung fluid at 37°C, size characterization of these particles is performed using DLS (NanoBrook 90Plus PALS analyzer) at designated time-intervals.

2.3 Effectiveness of PEGylation

2.3.1 Mucus penetration properties of TDNPs

A mucus permeation study was performed to study the effects of TDNPs in penetrating the mucus layer mimicking an *in vivo* condition (**Figure 5**). TDNPs loaded with Rhodamine B dye were used for the study. A 12-well transwell plate with a pore size of 0.8 μm was used for the study. Mucus was simulated based on previous literature[60]. Porcine mucin protein was mixed with salts and DPPC to form simulated mucus. 100μL of simulated mucus was placed on the transwell membrane and 500 μL of PBS was placed in the lower chamber. 25 μL of 10mg/mL of NPs were placed on top of the simulated mucus to allow permeation from the transwell to the lower chamber. PBS from the lower chamber was collected at various timepoints to measure the fluorescent NPs permeated through the mucus. Fresh PBS was replaced at different timepoints.

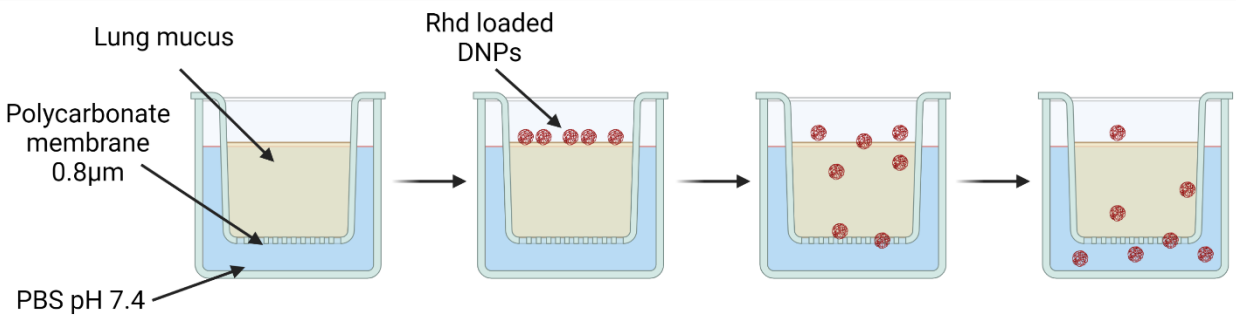

Figure 5: Schematic of mucus penetration setup

2.3.2 Collagen matrix penetration of TDNPs

A collagen matrix permeation study was performed to study the effects of TDNPs in penetrating the interstitial layer of the lung mimicking an *in vivo* condition. TDNPs loaded with Rhodamine B dye were used for the study. A 12-well transwell plate with a pore size of 0.8 µm was used for the study. Collagen matrix mimicking the interstitial layer was formed based on previous literature[61]. Collagen gel was prepared with 3 mg/mL Collagen Type 1. 100µL of collagen gel mixture was placed on the transwell membrane and incubated for 2 hours at 37°C. 500 µL of PBS was placed in the lower chamber. 25 µL of 10 mg/mL of NPs were placed on top of the collagen matrix for permeation from the transwell to the lower chamber. PBS from the lower chamber was collected at various timepoints to measure the fluorescent NPs permeated through the mucus. Fresh PBS was replaced at different timepoints.

2.4 *In vitro* evaluation of TDNPs

2.4.1 Cell culture

Human primary lung fibroblasts (HLF) were purchased through American Type Culture Collection (ATCC, Manassas, VA). Alveolar Type 1 (AT1) cells were purchased through Applied

Biological Materials Inc. (Richmond, BC, Canada). HLF cells were cultured in Fibroblast basal medium supplemented with 10% heat inactivated FBS. AT1 cells were cultured in IMDM medium supplemented with 10% heat inactivated FBS, 100 U/ml Penicillin. BT-20 cell lines were cultured in EMEM medium supplemented with 10% heat inactivated FBS, 100 U/ml Penicillin, and 100 µg/ml Streptomycin.

2.4.2 Myofibroblast induction of HLF cells

To induce fibrosis conditions *in vitro*, normal human lung fibroblasts (NHLFs; Lonza, Cat#: CC-2512) cells were induced with TGF-β. Briefly, cells seeded in a 6-well plate at 70% confluency were treated with 10 - 25 ng/ml of TGF-β in low serum media. The cells were washed after 48 hours, and α-SMA (fibrotic indicator) measured to confirm the induction of fibrotic cells. The expression of α-SMA was characterized by techniques including qPCR, Western Blot and Immunocytochemistry staining (ICC).

2.4.3 Pirfenidone IC50 Analysis

To test the effectiveness of the drug *in vitro,* IC50 analysis of the drug was performed on HLF cells that were induced with fibrosis via TGF-β. Briefly, HLF cells were seeded in a 24 well plate at 50% confluency. The cells were treated with 25 ng/mL of TGF-β in low serum media. After 24 hours of incubation, the cells were treated with varying concentrations of Pirfenidone (0-500 µg/mL). Cells were stained for αSMA protein expression at 48 hours after treatment and analyzed through fluorescent imaging. For quantitative assessment of the cells, we performed qPCR with the lysate and analyzed the αSMA gene expression. The effective concentration for the therapeutic studies would be chosen from this experiment.

2.4.4 Cytocompatibility of TDNPs

HLF & AT1 cells were seeded (5×10^3 cells/well) in 96-well plates and incubated overnight at 37°C. NPs were added at concentrations ranging from 0-500 μg/mL to the seeded cells. After incubation for 48 hours, cells were incubated with MTS reagent for one hour followed by measurement of the absorbance at 490 nm using an UV-Vis spectrophotometer (Tecan). Cell viabilities were calculated via normalizing to the control group (cells exposed to complete media only were considered having a 100% viability).

2.4.5 Targeting efficiency evaluation of TDNPs

To assess the targeting potential of TDNPs, fibrosis induced lung fibroblast cells (TGF-β treated) and healthy cells (non-treated) were incubated with dye (Rhodamine B)-loaded NPs (with and without the antibody conjugation) at similar concentrations for 2-4 hours, and the cells were washed carefully to remove the unbound NPs. The cells were washed twice and stained with NucBlue™ Live Cell Stain. After washing, cells were quantified via spectrophotometry, the TDNP amount in each sample was quantified via spectrophotometry and normalized with their respective NucBlue values. Furthermore, for visualizing the cellular uptake before the spectroscopic analysis, the cells were imaged using a fluorescent microscope (ECHO, San Francisco, CA) in the DAPI channel for nucleus and the Texas Red channel for NPs.

2.4.6 *In vitro* therapeutic effects of TDNPs

The therapeutic efficiency (anti-fibrotic efficiency) of the proposed TDNPs were assessed by determining their ability in inhibiting the upregulation of the α-SMA protein analyzed through qPCR. Briefly, HLF cells were seeded at 10,000 cells/well in a 96-well plate and treated with TGF-

β (10 ng/ml). After 24 hours, the cells were treated with the optimal NP concentration (obtained from the IC-50 study). This was done with the following control groups (individual free drug and no treatment) for the comparison of efficiency. The cells were treated for 48 hours with the NPs and then lysed and analyzed by western blotting for the expression of α-SMA levels. The groups were normalized to healthy HLF cells.

2.5 3D fibrosis model

2.5.1 Creation of a collagen-based 3D model

To create a 3D model of lung fibrosis, we modified and optimized based on an established dermal fibrosis model[61]. 3 mg/mL of acid soluble Type 1 collagen was used as the base material for the matrix. Briefly, 10,000 healthy HLF cells in 6.3 µL of 20% FBS complete media was added with 10 µL of 10X PBS and 0.4 µL of 1M NaOH. The solution was added and mixed to 33.3 µL of collagen (cold) and quickly added to a 96 well plate. The plate was incubated in 37°C for 2-3 hours and 100 µL of complete media was added to the well. After 24 hours of incubation, the cells were treated with 25 µg/mL of TGFβ. After 72 hours, the gel was stained with ICC staining for the expression of αSMA protein.

2.5.2 Therapeutic efficiency of TDNPs in 3D models

Once the 3D model was established, the therapeutic efficacy of the TDNPs were tested. Briefly, a cell matrix model was created in a 96 well plate and treated with TGFβ as discussed in **Section 2.5.1.** After 24 hours, the cells were treated with the optimal NP concentration (obtained from the IC-50 study). This was done with the following control groups (individual free drug and no treatment) for the comparison of efficiency. The cells were treated for 48 hours with the NPs

and then lysed and analyzed by western blotting for the expression of α-SMA levels. The groups were normalized to healthy HLF cells.

2.6 The evaluation of *in vivo* therapeutic & targeting effects of TDNPs

2.6.1 Creation of IPF mice

For *in vivo* evaluations, commonly used Bleomycin induced fibrosis model was used. To create the model, C57BL/6 mice were used as previously described in literature[62, 63]. Briefly, mice were anesthetized, and Bleomycin (2 U/kg body weight) dissolved in 50 µl of saline and injected through intratracheal intubation technique keeping the animal upright where it was slowly rotated for homogeneous distribution throughout the lung. 50 µl of saline was administered to the negative control group. After 21 days of Bleomycin administration, mice were scarified and histological evaluation on the lung sections were made to evaluate the pulmonary fibrosis. The extent of fibrosis induction was analyzed by H&E staining of the lung tissue for tissue scarring and Masson's trichrome staining for excess collagen formation in ECM.

2.6.2 Targeting and retention study on IPF mice

To analyze the nanoparticle formulations targeting capability to assess the tissue/organ, we performed a biodistribution study in mice. For this initial study, we used the mice strain of 7–10-week old C57BL/6J mice (both sexes). The mice were induced with IPF as discussed in **Section 2.6.1**. Florescent dye-labeled nanoparticle formulations with concentration of 5 mg/mL were nebulized using an aeroneb® lab module nebulizer. Saline solution nebulization was used as negative control. After 3 hours of nebulization, mice were euthanized by CO2 inhalation, followed by whole body and organ fluorescence imaging (Kodak in vivo imaging FX Pro- LS Rm554) to

assess biodistribution profiles. The lung tissues were extracted and sliced using cryostat sectioning techniques. The sections were stained using NucBlue™ Live Cell Stain. The tissues were analyzed using fluorescent microscopy to analyze the enhanced uptake and retention of TDNPs compared to PLGA NPs.

2.6.3 Investigation of the *in vivo* effectiveness of TDNPs on IPF mice

To evaluate the efficacy of nanoparticle formulation on treating fibrosis in, we carried out a proof-of-concept study to assess whether nanoparticle formulation could be used to treat fibrosis and cure scar tissue in the lung (**Figure 6**). For this study, 7–10-week old C57BL/6J mice (both sexes) were used. The mice were induced with Bleomycin to form IPF as discussed in **Section 2.6.1**

Three days (72 hours) after Bleomycin intubation, mice were administered with either saline, free drug or antifibrotic nanoparticle formulation via nebulization (same procedure as biodistribution studies) with an experiment timeline shown below.

After 14 days, mice were euthanized, organs and blood were collected via sterile necropsy and heart puncture, respectively. Histological analysis of lungs, and tissue damage in lungs were assessed. These assessments were used to determine the therapeutic efficacy of nanoformulations.

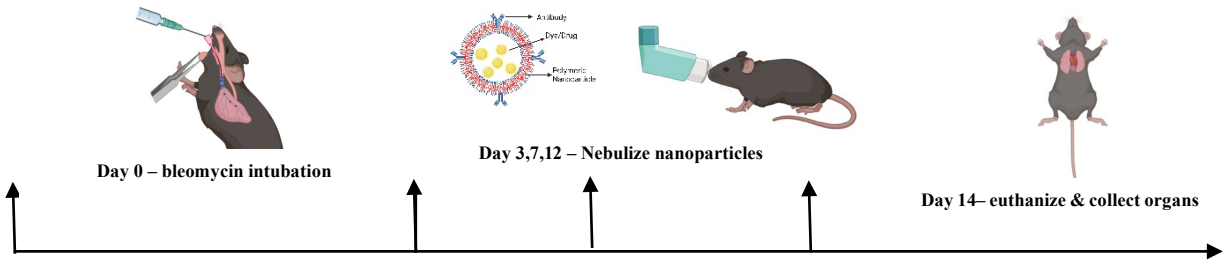

Figure 6. Timeline of *in vivo* therapeutic efficiency study

2.7 Statistical analysis

GraphPad Prism 8 (GraphPad Software Inc., San Diego, USA) was used to perform statistical analysis. One-way ANOVA with Dunnett multiple comparisons and Tukey's multiple comparison tests were done for all the analyses. Triplicate samples were used for all the studies if not specified.

Chapter 3

RESULTS AND DISCUSSION

3.1 TDNP fabrication and characterization

3.1.1 TDNPs fabrication and characterization

In this study, we prepared biodegradable PLGA-PEG nanoparticles as a high efficiency mucus penetrating drug delivery system. The prepared NPs were ~380 nm, which is ideal for intratracheal delivery for the lower respiratory track as it avoids exhalation and accumulation in the upper respiratory track[29]. The particles were also tested for their Zeta potential charge (**Figure 7B**), we

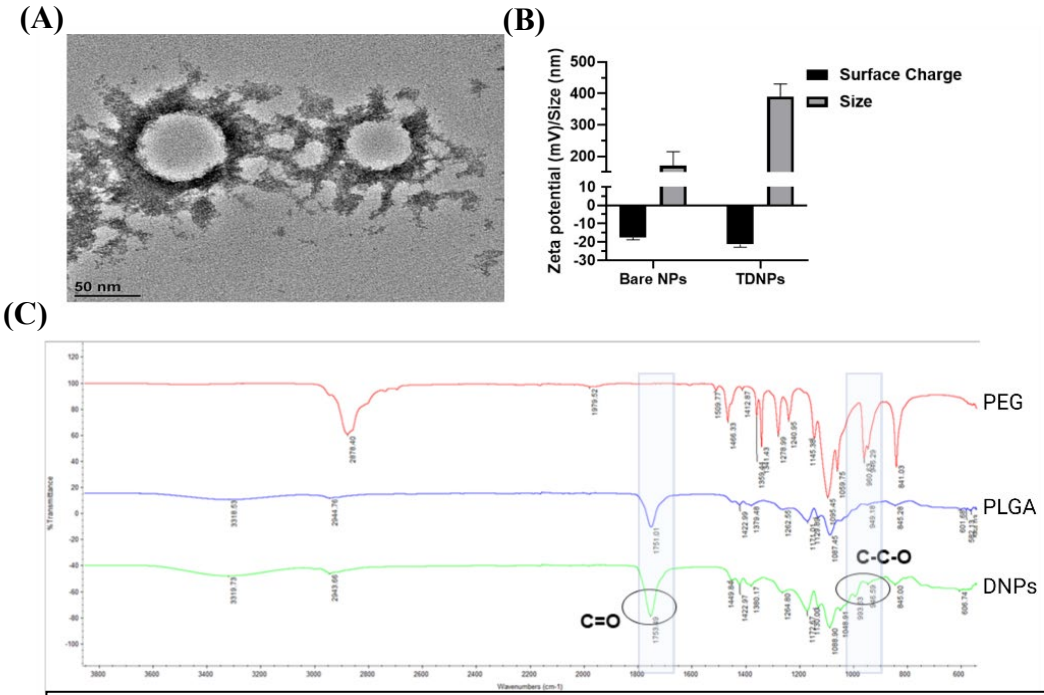

Figure 7. Physicochemical characteristics of TDNPs. A. TEM image of the TDNPs showing their spherical shape and the PEG molecules on the surface of the particles. **B.** DLS measurement of bare NP and TDNP. We can observe that the size after drug loading and conjugation has increased by almost double; we can also see that there is not a big difference in ZETA potential value, with TDNPs being highly stable. **C.** FTIR spectra of DNPs show a significant peak at 1752 cm^{-1} which is a characteristic peak of PLGA' C=O stretching. A small peak around 950 and 840 cm^{-1} is also observed confirming the presence of PEG.

observed that TDNPs had a charge of ~ -20mV denoting that the particles were very stable with very less chance of aggregation.

To confirm the presence of the PEG layer on the polymersome, FTIR was performed to detect the presence of functional groups (**Figure 7C**). We observed the characteristic peak at 1752 cm^{-1} was attributed to the C=O stretching and is clearly observed in the PLGA and PLGA-PEG spectra. We can also see that the NPs show a small signal around 950 and 840 cm^{-1}, that attributes to the C-C-O harmonica, denoting the presence of PEG on the surface[64].

3.1.2 Drug release profiles

The drug release kinetics of the NPs were analyzed for their applications in therapeutic studies. NPs at a concentration of 2 mg/mL were used for drug release analysis. The study was performed at 37°C in 1X PBS (pH 7.4) at different time points. The release rate of the nanoparticles is shown in **Figure 8**. We observed that NPs had a burst release of ~17 % in the first 6 hours, followed by a sustained release phase up to 3 days.

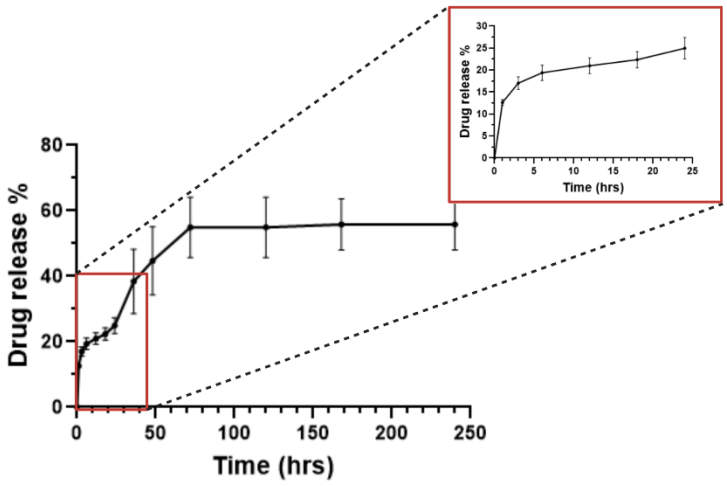

Figure 8. Drug release profile of TDNPs

3.1.3 TDNPs stability

The stability analysis of the bare NPs and drug loaded TDNPs were analyzed for an extended time of 72 hours in simulated lung fluid (Fisher Scientific) at 37°C. The simulated lung fluid represents the interstitial fluid deep within the lung acting as a mimic of *in vivo* conditions. Both the blank and drug loaded NPs had no significant change in their size for the whole length of the experiment (**Figure 9**). Though there was a slight increase in the size of the NPs after 24 hours, the change was not significant. There was no sign of aggregation of the NPs during the study, attesting to their stability.

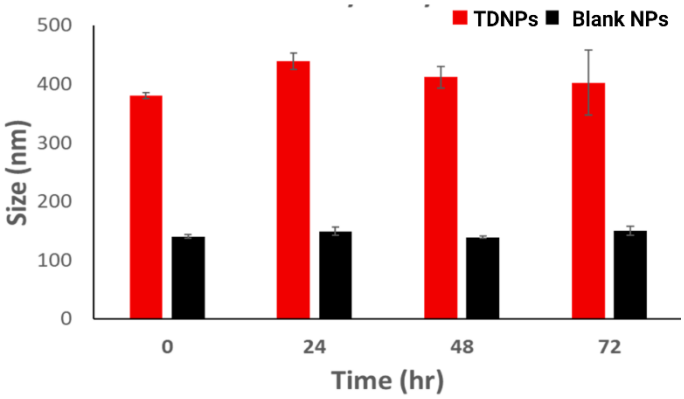

Figure 9. Stability study of TDNPs shows no significant change in size over 72 hours.

3.2 Mucus & matrix penetration studies of TDNPs

The mucus layer is a key barrier in the delivery of drugs and drug carriers intratracheally[65, 66] because the complex barrier becomes more viscous and adherent during IPF[67, 68]. It is, thus, vital to study the mucus penetrating capability of nanoparticles. Recent reports suggest that nanoparticles <500 nm with a mucus inert coating can navigate through the mucus layer[69]. In this experiment, we assessed the effectiveness of the PEGylated NPs in penetrating the mucus layer compared to plain PLGA NPs. Nanoparticles labeled with Rhodamine B were layered on top of simulated mucus, and their permeation through mucus and a 0.8 μm pore size transwell into the lower chamber was recorded to assess permeation kinetics. We observed that PEGylated NPs (or TDNPs) had a significantly higher mucus penetration compared to that of plain PLGA NPs (**Figure 10**). We observed that even starting from a 3 hours timepoint, the rate of mucus penetration was significantly higher for TDNPs compared to that of PLGA NPs. This clearly shows that the PEGylation of NPs provide enhanced penetration through mucus, and the TDNPs would act as an ideal drug carrier for intratracheal drug delivery, especially for lung fibrosis.

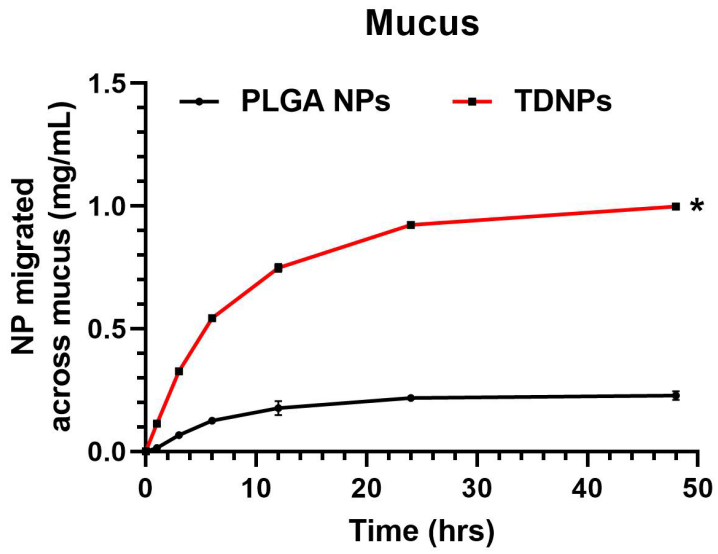

Figure 10. Mucus penetration study of TDNPs. TDNPs have higher rates of mucus penetration compared to the PLGA NPs throughout the experiment timepoint *(*P<0.05)*.

Once the NPs cross the mucus layer, they still have to penetrate the thick collagen matrix to reach the myofibroblast. Since during tissue scarring, the collagen production rate greatly exceeds the collagen degradation rate, there is accumulation of fibrillar collagen in the extracellular matrix[70]. The NPs were thus tested in their efficiency to cross the *in vivo* mimicking collagen matrix. We observed that the PEGylated NPs showed higher matrix penetration compared to that of PLGA NPs. The rate of NP penetration was significantly higher for the TDNPs throughout the experimental timepoint (**Figure 11**). Both the mucus penetration and collagen matrix penetration show the potential of PEGylation in intratracheal delivery of drugs and its ability to reach and deliver drugs to the damaged myofibroblasts.

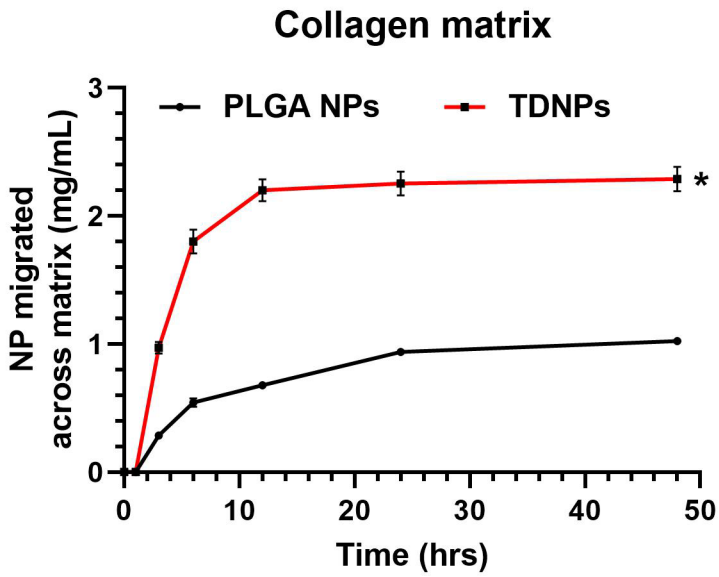

Figure 11. Collagen matrix penetration study of TDNPs TDNPs have a higher rate of penetration compared to the PLGA NPs throughout the experiment timepoint. *(*P<0.05)*

3.3 *In vitro* studies of TDNPs

3.3.1 Disease establishment in 2D model

A fibrosis condition was induced in the healthy human lung fibroblast (HLF) cells by treating them with TGF β1 as briefly described in the experiment section. Immunocytochemistry (ICC) was performed on these treated cells with α-SMA protein as a marker of fibrosis. We used α-SMA antibody conjugated with Texas Red to determine the level of protein induction in terms of fibrosis

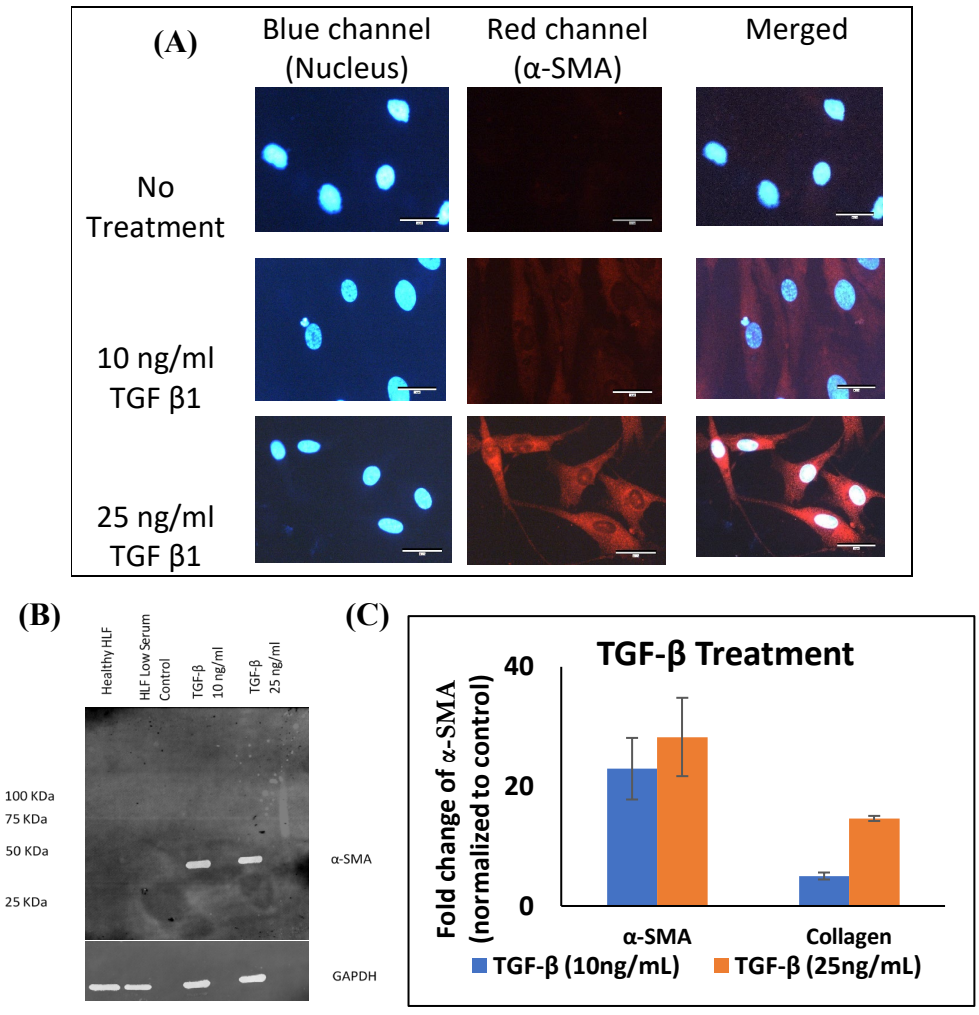

Figure 12. **Fibrosis establishment in 2D model A.** ICC staining of HLF with DAPI (Blue) nuclear staining and Texas Red α-SMA protein (Red) staining after treatment with TGF β1. **B.** Western Blot with α-SMA antibody. **C.** RT-qPCR data, quantifying the induction of Fibrotic cells by TGF-β Treatment.

induction. We observed that cells treated with both 10 and 25 ng/ml turned the cells fibrotic with

25 ng/ml being more prominent (**Figure 12A**). The induction of fibrosis is also quantified by the amount of α-SMA protein and collagen-1 protein expression using Western Blot and their respective RNA values using the RT-qPCR. We observed that there was more than a 20-fold increase in the α-SMA expression for even 10 ng/ml TGF-β treatment and 30-fold for 25 ng/ml of TGF-β (**Figure 12B**). We observed a similar trend in the collagen-1 expression, which signifies a successful transformation of healthy HLF into fibrotic cells via TGF-β treatment. We also observed a clear band at 42 KDa for both TGF β1 concentrations, with 25 ng/ml having a slightly higher concentration of proteins (**Figure 12C**). Though both concentrations produced fibrotic conditions, 25 ng/ml was used for further studies as it showed more prominent expression of α-SMA protein in both the studies.

3.3.2 IC_{50} analysis of Pirfenidone

The effective concentration dose of Pirfenidone as a drug to treat TGFβ induced fibrosis was analyzed. The cells induced with TGFβ were treated with different concentrations of Pirfenidone (0-500 μg/mL) to determine the effective dose range for therapeutic studies. The cells after treatment were analyzed by ICC staining for the presence of α-SMA protein (similar procedure as Section 3.3.1). We observed that at concentration 10 μg/mL, though the expression of α-SMA protein was reduced, significant expression of α-SMA protein was observed (**Figure 13A**). We observed that for concentrations 50-100 μg/mL, there was negligible to no visible expression of α-SMA protein. However, at a concentration of 500 μg/mL, we again observed significant expression of α-SMA protein. The results were quantitatively confirmed through qPCR analysis of the cell lysate, where we observed that only for the concentration range of 50-100 μg/mL did we observe significant reduction in the α-SMA gene expression (**Figure 13B**). Though there was

a reduction in expression of the α-SMA gene in the concentration of 10 & 500 µg/mL, it was not significant. Thus, the concentration range of 50-100 µg/mL would be used for further therapeutic

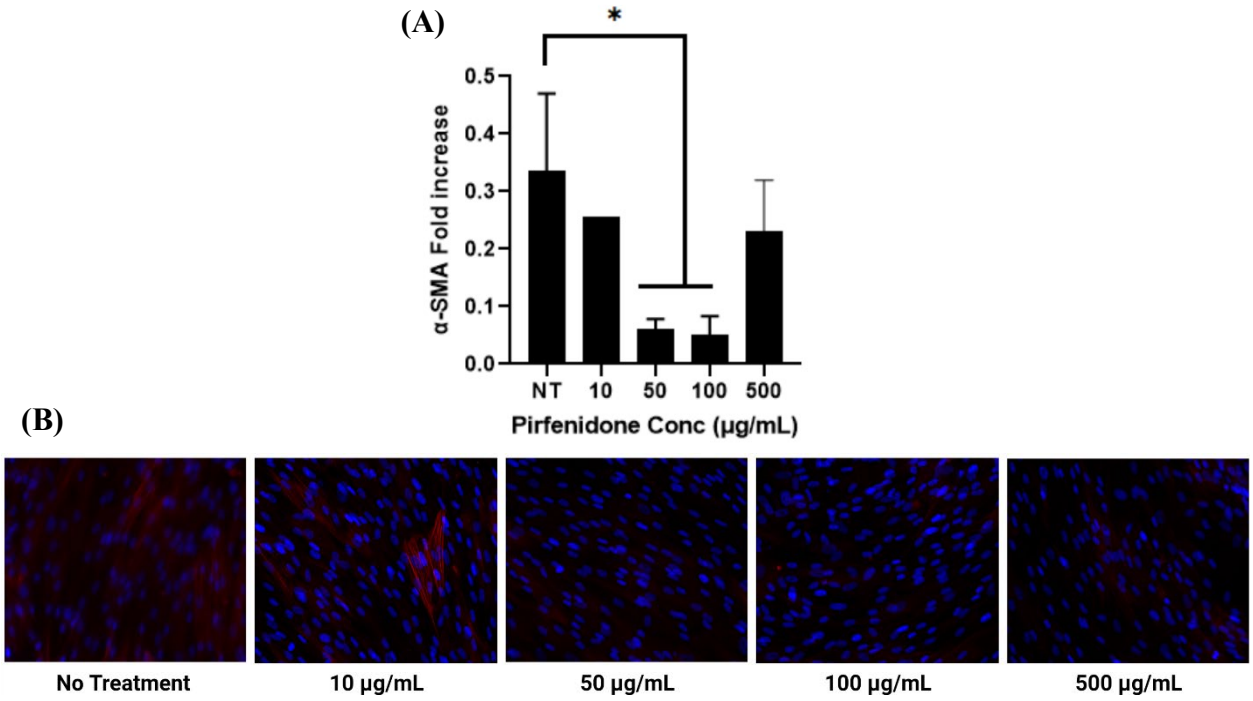

Figure 13. IC50 Analysis of Pirfenidone by **A.** qPCR quantitative analysis. **B.** ICC staining of HLF with DAPI (Blue) nuclear staining and Texas Red α-SMA protein (Red) staining on TGFβ induced HLF cells.

efficiency studies.

3.3.3 Cytocompatibility analysis of TDNPs

The cytocompatibility of the TDNPs and blank NPs were analyzed up to 500 mg/mL in healthy lung epithelial (AT1) cells and healthy lung fibroblast (HLF) cells. The viability of the cells was normalized to untreated healthy cells. We observed no significant reduction in viability throughout the concentration of cells compared to no treatment (**Figure 14**). We observed no significant change in viability observed between the blank NPs and the TDNPs group. The NPs are thus biocompatible for an extended concentration of 0 - 500 mg/mL with no observable toxicity.

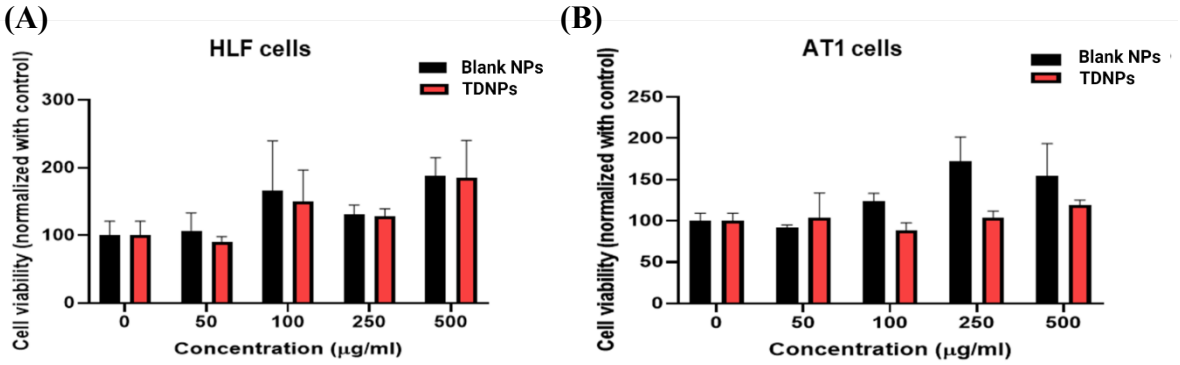

Figure 14. Cytocompatibility of TDNPs on **A.** HLFs and **B.** AT1 healthy cells. Cell viability was analyzed by MTS assays, and it showed no inherent toxicity to the cells.

3.3.4 TDNPs uptake study

The targeting and uptake efficiency of FAP antibody conjugated NPs (TDNPs) were analyzed and compared with untargeted NPs. Dye (Coumarin 6) loaded nanoparticles were used for the study. The fibrosis induced cells were treated with nanoparticles for 3 hours, washed and imaged under fluorescent microscope (**Figure 15A**). We observed that FAP targeted nanoparticles showed higher uptake (green color) compared to that of unconjugated NPs, attesting to the necessity and effectiveness of active targeting through FAP antibodies. The cells were lysed and analyzed quantitatively through spectroscopy (**Figure 15B**). We observed that the spectroscopic data aligned with the microscopy data where the TDNPs had significantly higher uptake compared to that of DNPs.

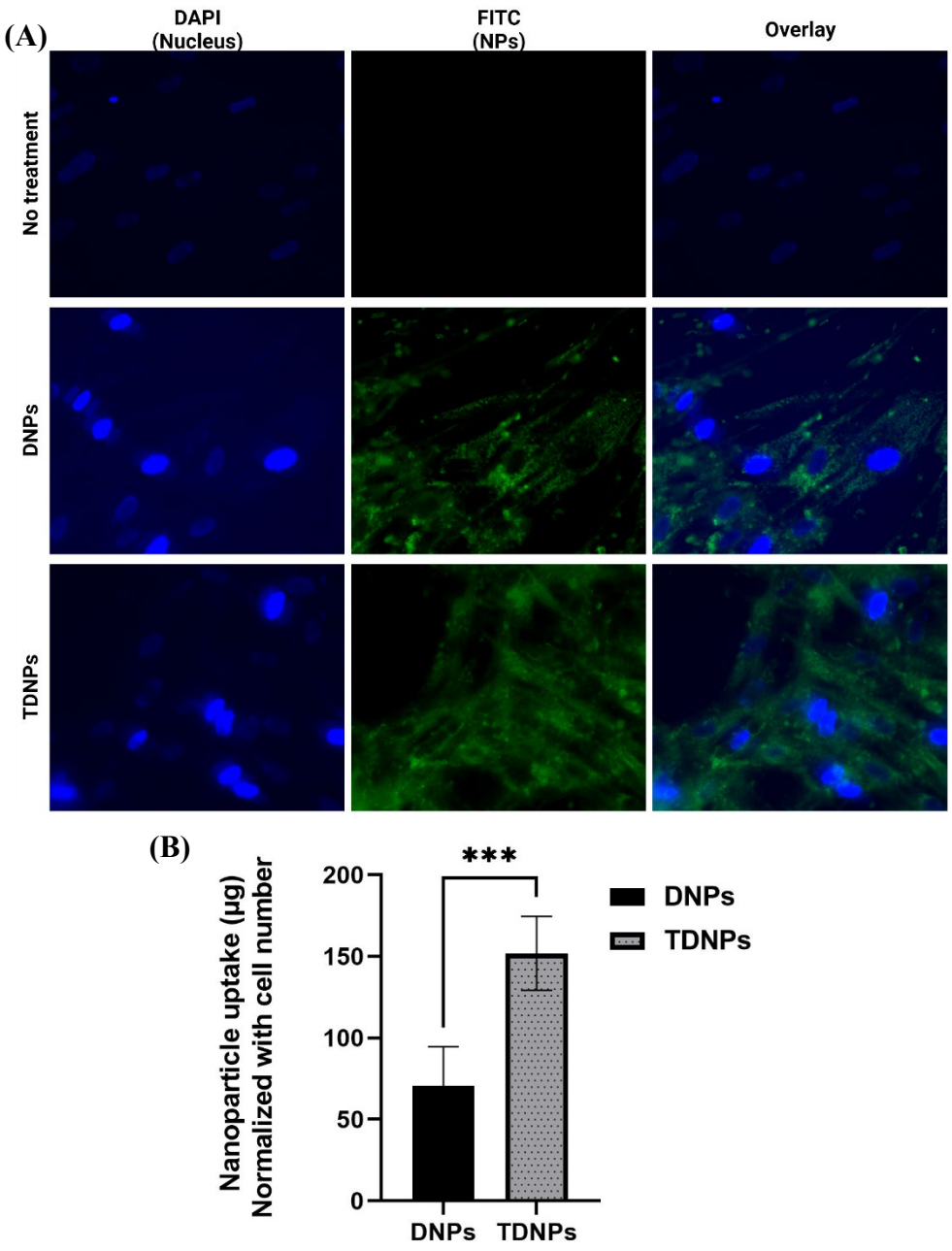

Figure 15. Targeting efficiency of TDNPs analyzed by **A.** Fluorescent microscopy shows significantly higher uptake of NPs (green) in TDNPs group compared to that of DNPs. **B.** Quantitative spectroscopy analysis of cell lysis also shows significantly higher uptake and retention of TDNPs compared to that of DNPs. *(***$p<0.001$).*

3.3.5 *In vitro* therapeutic effects of TDNPs

The therapeutic efficiency of TDNPs was analyzed *in vitro* by analyzing its effectiveness in reducing the expression of α-SMA gene via qPCR. The TDNPs were compared with free Pirfenidone and no treatment control. The Pirfenidone amount was kept constant for both the groups. We observed that the TDNPs reduced the α-SMA expression significantly compared to that of both the control and free drug (**Figure 16**). We observed a 10-fold increase in α-SMA expression in the free drug compared to a 20-fold increase in the no treatment group. This was further reduced to less than a 5-fold increase in the TDNP group. This result clearly shows the necessity and effectiveness of a targeted drug delivery system to treat fibrosis.

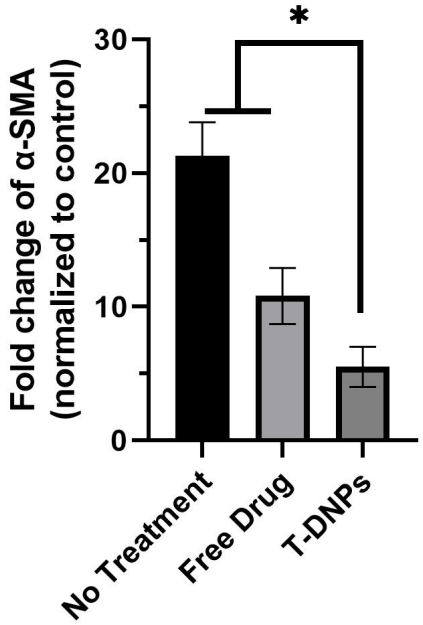

Figure 16. Therapeutic efficiency of TDNPs analyzed by quantitative qPCR data shows significant reduction in the αSMA gene expression in the TDNP group compared to that of free drug. *(*P<0.05)*

3.4 3D fibrosis model

The collagen matrix after 72 hours of TGFβ was stained using ICC staining for analyzing the presence of αSMA protein (red) as an indicator for fibrosis. The samples were imaged using confocal microscopy with Z thickness of 16µm (**Figure 17**). We observed that even with the thickness of the gel, most of the cells inside the matrix have been induced with fibrosis as seen by the expression of αSMA protein (red). We observed that most of the cells were expressing αSMA filament, even better than that of the 2D model.

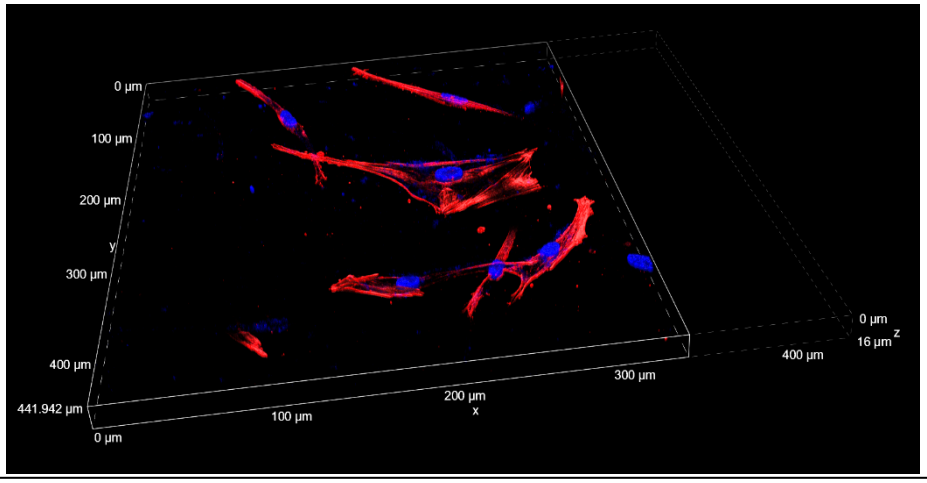

Figure 17. Confocal image of fibrotic region in TGFβ induced 3D collagen matrix. Observed αSMA protein (red) expression in almost all cells through the thickness of the matrix.

3.4.1 Therapeutic effect of TDNPs in 3D fibrosis model

The therapeutic efficiency of TDNPs was analyzed in the created 3D fibrosis model by analyzing its effectiveness in reducing the expression of the α-SMA gene via qPCR. The TDNPs were compared with free Pirfenidone and no treatment control. The Pirfenidone amount was kept constant for both the groups. We observed that the TDNPs reduced the α-SMA expression significantly compared to that of both the control and free drug (**Figure 18**). We observed a 13-fold increase in α-SMA expression in the free drug compared to an 18-fold increase in the no treatment group. This was further reduced to less than a 6-fold increase in the TDNP group. This

result clearly shows the necessity and effectiveness of a targeted drug delivery system to treat fibrosis.

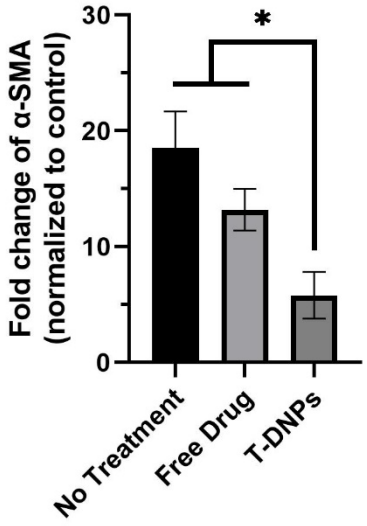

Figure 18. Therapeutic efficiency of TDNPs in 3D fibrotic model analyzed by quantitative qPCR data shows significant reduction in the αSMA gene expression in the TDNPs group compared to that of free drug. *(*P<0.05)*

3.5 *In vivo* studies of TDNPs

3.5.1 IPF models

An idiopathic pulmonary fibrosis model was created in the mice following a well-established protocol. Briefly, the mice were injected with 2 U/kg of Bleomycin via intratracheal intubation. The mice were housed under monitoring for 14 days. After 14 days, the lung tissues were analyzed by both H&E staining and Mason's trichrome staining to verify the extent of tissue damage and collagen accumulation, respectively. This would be the direct indicator of Fibrosis. The H&E staining done on the lung tissues of the Bleomycin injected mice clearly showed rigidity of lung tissue compared to that of the saline group (**Figure 19A**). We can clearly see the alveolar structure in the saline group which has disappeared almost completely in the Bleomycin group. The tissues were graded by standard Ashcroft's scale, and we observed that the Bleomycin injected mice had

a score of 6-7 compared to 0-1 on the saline. The Bleomycin mice's score was significantly higher than that of saline (**Figure 19B**).

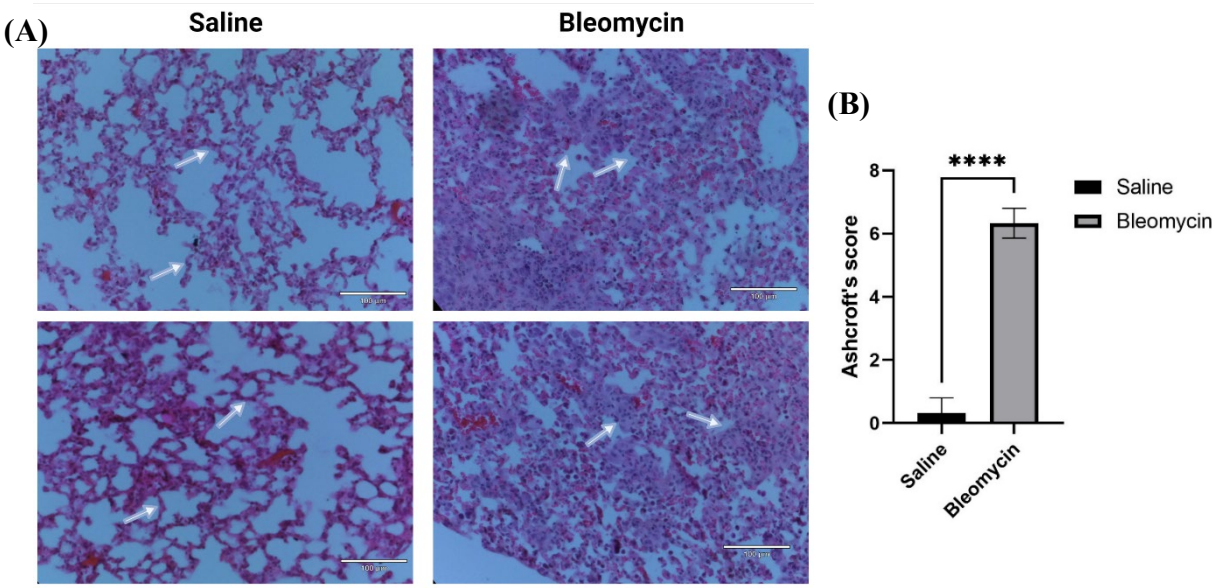

Figure 19. Lung tissue of Bleomycin induced IPF model A. Hemoxylin and Eosin staining of paraffin-embedded lung tissues. Bleomycin treated group had a high density of fibrotic tissues and scarring. No significant tissue damage was seen in the saline group. **B.** Ashcroft's scoring of the lung tissue shows significant increase in the Bleomycin group compared to saline.

The tissues were further analyzed with Masson's trichrome staining to quantify the collagen expression and deposition. Masson's trichrome stains the collagen in the tissue blue. We observed that the Bleomycin injected mice had a high deposition of collagen (**Figure 20**). Through color deconvolution software, we analyzed the area covered with collagen, eliminating the other tissues. We observed that the Bleomycin injected mice had significantly higher collagen deposited areas compared to that of saline. Through these experiments, we showed that the model was successfully established, and the same procedure would be used for therapeutic and NP retention studies.

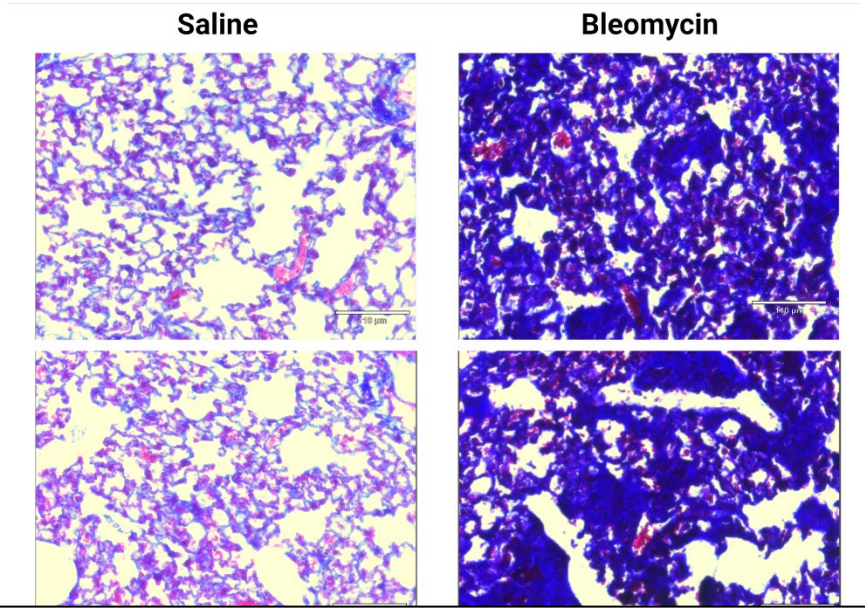

Figure 20. Masson's trichrome staining of lung tissue of Bleomycin induced IPF model. Bleomycin group had significantly higher deposition of collagen (Blue).

3.5.2 Targeting and retention study of TDNPs on IPF mice

TDNPs' ability to target fibrotic and ability to get uptaken was analyzed using Rhodamine B loaded TDNPs and was compared with plain PLGA NPs. The nanoparticles were nebulized, and after 3 hours, the mice were euthanized. The lung tissues were collected, washed, sliced and imaged under fluorescent microscopy (**Figure 21**). The tissue was stained with nuclear stain (blue) to show the cellular structure. We observed that the accumulation and uptake of TDNPs was significantly higher than that of PLGA NPs. The results indicate that TDNPs were able to reach the alveolar region, and that PEG helps in penetration of NPs in the lung tissues.

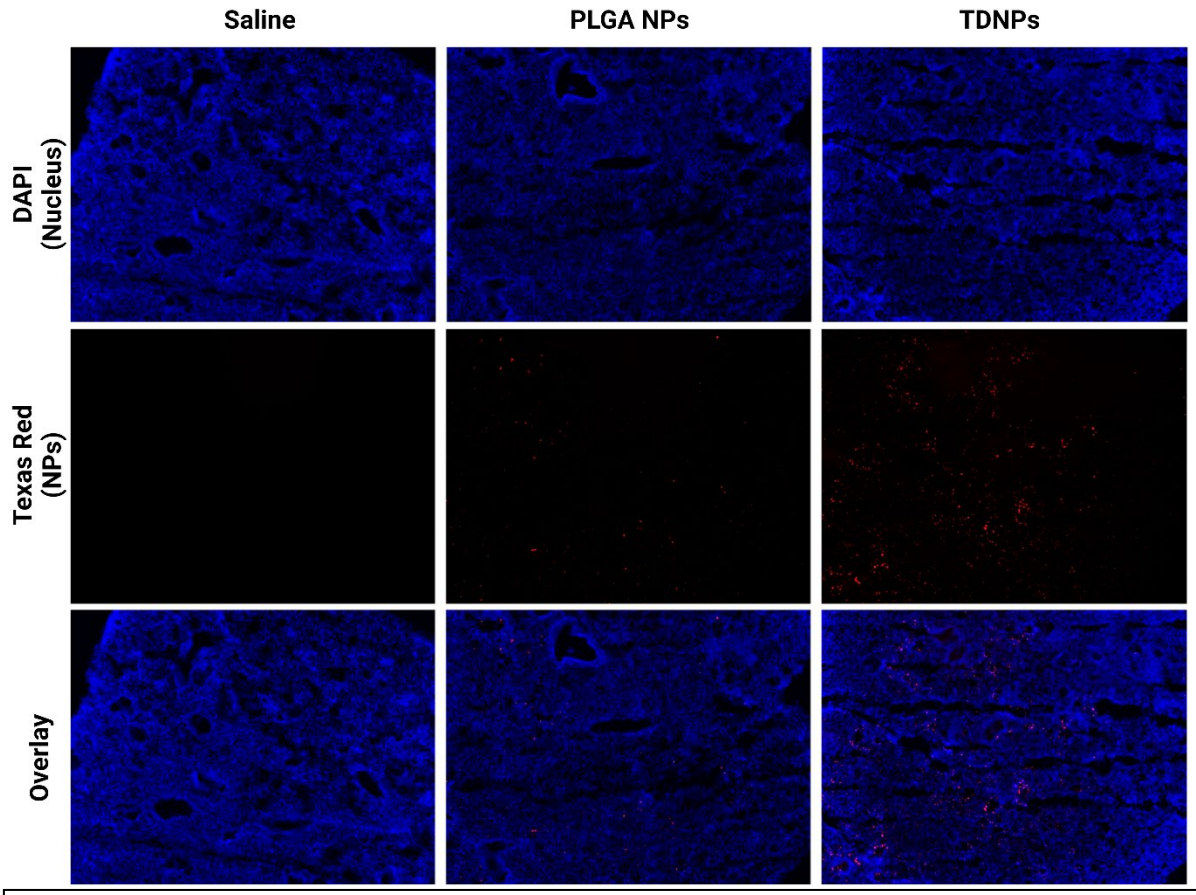

Figure 21. Targeting and retention efficiency of TDNPs was analyzed by fluorescent microscopy of tissue sections. We saw significantly higher accumulation and retention of NPs (red) in the TDNPs group compared to that of the PLGA group.

Chapter 5

Conclusion

To summarize, we developed a novel nanoparticle drug delivery system that could penetrate lung mucosa and target the damaged myofibroblast to deliver drugs in the fibrotic region. The NPs were characterized for their optimal size < 500nm to reach the deep alveolar regions and consisted of their stability in the stimulated lung fluid. They had a very high cytocompatibility to healthy cells and provided a sustained drug release. The NPs with the PEG surface showed enhanced simulated mucus and collagen matrix penetration, indicating its ability to deliver drugs to fibrotic lung cells. We were successfully able to create 2D and 3D models of fibrosis for *in vitro* studies to test our NPs for their therapeutic efficiency. We showed that our NPs had significantly higher therapeutic efficiency compared to that of free Pirfenidone.

We created a lung model in mice that was comparable and pathologically similar to clinical disease. We also showed the efficiency of our NPs' localization and retention capabilities to lung tissues in this mouse model. These results support our hypothesis that the targeted PLGA-PEG based polymersomes can act as a potential drug delivery system to target and treat pulmonary fibrosis.

Chapter 6

Limitations and Future Work

Although our findings show high efficiency in inhalation delivery of nanoparticles and therapeutic efficiency of our TDNPs in delivering a drug to diseased lung tissues and treating lung fibrosis, there are a few limitations that have to be addressed. Since fibrosis is a relatively new field, there is a lack of clinically approved drugs that can reverse late-stage fibrosis. This makes the proposed NPs optimal for early to mid-stage fibrosis. Though this is a current limitation, the proposed NP is a universal design which can carry any new drugs that are created in the future to increase its efficiency.

Though the 3-D model created was able to bring us closer to the interstitial region of fibrotic tissues, more optimized design is essential that provides layered interaction between the epithelial and interstitial layer.

A more integrated "organ-on-chip" is being designed in collaboration with Dr. Yang, with the data produced in this thesis, could provide a more robust design to create a 3D fibrosis model that completely mimics a clinical model in every aspect. The proposed NP system can be used for many applications including lung infections and cystic fibrosis that has mucus accumulation as a barrier for drug delivery.

Based on our encouraging results, future therapeutic studies in mice models with pulmonary fibrosis with various dosages should be performed to assess the optimal dose and clinical potential of a targeted drug delivery system.

References

1. Álvarez, D.; Levine, M.; Rojas, M., Regenerative medicine in the treatment of idiopathic pulmonary fibrosis: current position. (1178-6957 (Print)).
2. Liu, Y.-M.; Nepali, K.; Liou, J.-P., Idiopathic Pulmonary Fibrosis: Current Status, Recent Progress, and Emerging Targets. *Journal of Medicinal Chemistry* **2017,** *60* (2), 527-553.
3. Kreuter, M.; Bonella, F.; Wijsenbeek, M.; Maher, T. M.; Spagnolo, P., Pharmacological Treatment of Idiopathic Pulmonary Fibrosis: Current Approaches, Unsolved Issues, and Future Perspectives. *BioMed Research International* **2015,** *2015*, 329481.
4. Krishna R Fau - Chapman, K.; Chapman, K.; Ullah, S., Idiopathic Pulmonary Fibrosis. BTI - StatPearls.
5. Spagnolo, P.; Tonelli R Fau - Cocconcelli, E.; Cocconcelli E Fau - Stefani, A.; Stefani A Fau - Richeldi, L.; Richeldi, L., Idiopathic pulmonary fibrosis: diagnostic pitfalls and therapeutic challenges. (2049-6958 (Electronic)).
6. Spagnolo, P.; Tzouvelekis, A.; Bonella, F., The Management of Patients With Idiopathic Pulmonary Fibrosis. (2296-858X (Print)).
7. Glass, D. S.; Grossfeld, D.; Renna, H. A.; Agarwala, P.; Spiegler, P.; DeLeon, J.; Reiss, A. B., Idiopathic pulmonary fibrosis: Current and future treatment. *The Clinical Respiratory Journal* **2022,** *16* (2), 84-96.
8. Martinez, F. J.; Collard, H. R.; Pardo, A.; Raghu, G.; Richeldi, L.; Selman, M.; Swigris, J. J.; Taniguchi, H.; Wells, A. U., Idiopathic pulmonary fibrosis. *Nature Reviews Disease Primers* **2017,** *3* (1), 17074.
9. Kistler, K. D.; Nalysnyk L Fau - Rotella, P.; Rotella P Fau - Esser, D.; Esser, D., Lung transplantation in idiopathic pulmonary fibrosis: a systematic review of the literature. (1471-2466 (Electronic)).
10. Weill, D.; Benden, C.; Corris, P. A.; Dark, J. H.; Davis, R. D.; Keshavjee, S.; Lederer, D. J.; Mulligan, M. J.; Patterson, G. A.; Singer, L. G.; Snell, G. I.; Verleden, G. M.; Zamora, M. R.; Glanville, A. R., A consensus document for the selection of lung transplant candidates: 2014--an update from the Pulmonary Transplantation Council of the International Society for Heart and Lung Transplantation. (1557-3117 (Electronic)).
11. Somogyi, V.; Chaudhuri, N.; Torrisi, S. E.; Kahn, N.; Müller, V.; Kreuter, M., The therapy of idiopathic pulmonary fibrosis: what is next? *European Respiratory Review* **2019,** *28* (153), 190021.
12. Riddell, P.; Kleinerova, J.; Eaton, D.; Healy, D. G.; Javadpour, H.; McCarthy, J. F.; Nolke, L.; Redmond, K. C.; Egan, J. J., Meaningful survival benefit for single lung transplantation in idiopathic pulmonary fibrosis patients over 65 years of age. *European Respiratory Journal* **2020,** *56* (1), 1902413.
13. Shivaswamy, V.; Boerner, B.; Larsen, J., Post-Transplant Diabetes Mellitus: Causes, Treatment, and Impact on Outcomes. (1945-7189 (Electronic)).
14. Le Pavec, J.; Dauriat, G.; Gazengel, P.; Dolidon, S.; Hanna, A.; Feuillet, S.; Pradere, P.; Crutu, A.; Florea, V.; Boulate, D.; Mitilian, D.; Fabre, D.; Mussot, S.; Mercier, O.; Fadel, E., Lung transplantation for idiopathic pulmonary fibrosis. *La Presse Médicale* **2020,** *49* (2), 104026.
15. Li, D.; Liu, Y.; Wang, B., Single versus bilateral lung transplantation in idiopathic pulmonary fibrosis: A systematic review and meta-analysis. *PLOS ONE* **2020,** *15* (5), e0233732.

16. Myllärniemi, M.; Kaarteenaho, R., Pharmacological treatment of idiopathic pulmonary fibrosis – preclinical and clinical studies of pirfenidone, nintedanib, and N-acetylcysteine. *European Clinical Respiratory Journal* **2015,** *2* (1), 26385.
17. Bargagli, E.; Piccioli, C.; Rosi, E.; Torricelli, E.; Turi, L.; Piccioli, E.; Pistolesi, M.; Ferrari, K.; Voltolini, L., Pirfenidone and Nintedanib in idiopathic pulmonary fibrosis: Real-life experience in an Italian referral centre. *Pulmonology* **2019,** *25* (3), 149-153.
18. Noble, P. W.; Albera, C.; Bradford, W. Z.; Costabel, U.; du Bois, R. M.; Fagan, E. A.; Fishman, R. S.; Glaspole, I.; Glassberg, M. K.; Lancaster, L.; Lederer, D. J.; Leff, J. A.; Nathan, S. D.; Pereira, C. A.; Swigris, J. J.; Valeyre, D.; King, T. E., Pirfenidone for idiopathic pulmonary fibrosis: analysis of pooled data from three multinational phase 3 trials. *European Respiratory Journal* **2016,** *47* (1), 243.
19. King, T. E.; Bradford, W. Z.; Castro-Bernardini, S.; Fagan, E. A.; Glaspole, I.; Glassberg, M. K.; Gorina, E.; Hopkins, P. M.; Kardatzke, D.; Lancaster, L.; Lederer, D. J.; Nathan, S. D.; Pereira, C. A.; Sahn, S. A.; Sussman, R.; Swigris, J. J.; Noble, P. W., A Phase 3 Trial of Pirfenidone in Patients with Idiopathic Pulmonary Fibrosis. *New England Journal of Medicine* **2014,** *370* (22), 2083-2092.
20. Cameli, P.; Refini, R. M.; Bergantini, L.; d'Alessandro, M.; Alonzi, V.; Magnoni, C.; Rottoli, P.; Sestini, P.; Bargagli, E., Long-Term Follow-Up of Patients With Idiopathic Pulmonary Fibrosis Treated With Pirfenidone or Nintedanib: A Real-Life Comparison Study. *Frontiers in Molecular Biosciences* **2020,** *7*.
21. Verma, N.; Kumar, P.; Mitra, S.; Taneja, S.; Dhooria, S.; Das, A.; Duseja, A.; Dhiman, R. K.; Chawla, Y., Drug idiosyncrasy due to pirfenidone presenting as acute liver failure: Case report and mini-review of the literature. *Hepatology Communications* **2018,** *2* (2), 142-147.
22. Lamb, Y. N., Nintedanib: A Review in Fibrotic Interstitial Lung Diseases. *Drugs* **2021,** *81* (5), 575-586.
23. Richeldi, L.; du Bois, R. M.; Raghu, G.; Azuma, A.; Brown, K. K.; Costabel, U.; Cottin, V.; Flaherty, K. R.; Hansell, D. M.; Inoue, Y.; Kim, D. S.; Kolb, M.; Nicholson, A. G.; Noble, P. W.; Selman, M.; Taniguchi, H.; Brun, M.; Le Maulf, F.; Girard, M.; Stowasser, S.; Schlenker-Herceg, R.; Disse, B.; Collard, H. R., Efficacy and Safety of Nintedanib in Idiopathic Pulmonary Fibrosis. *New England Journal of Medicine* **2014,** *370* (22), 2071-2082.
24. Hirani, N.; MacKinnon, A. A.-O.; Nicol, L.; Ford, P.; Schambye, H.; Pedersen, A.; Nilsson, U. J.; Leffler, H.; Sethi, T.; Tantawi, S.; Gravelle, L. A.-O. X.; Slack, R. J.; Mills, R.; Karmakar, U.; Humphries, D. A.-O.; Zetterberg, F. A.-O.; Keeling, L.; Paul, L.; Molyneaux, P. A.-O.; Li, F. A.-O.; Funston, W.; Forrest, I. A.; Simpson, A. A.-O.; Gibbons, M. A.; Maher, T. M., Target inhibition of galectin-3 by inhaled TD139 in patients with idiopathic pulmonary fibrosis. LID - 10.1183/13993003.02559-2020 [doi] LID - 2002559. (1399-3003 (Electronic)).
25. Desroy, N.; Housseman, C.; Bock, X.; Joncour, A.; Bienvenu, N.; Cherel, L.; Labeguere, V.; Rondet, E.; Peixoto, C.; Grassot, J.-M.; Picolet, O.; Annoot, D.; Triballeau, N.; Monjardet, A.; Wakselman, E.; Roncoroni, V.; Le Tallec, S.; Blanque, R.; Cottereaux, C.; Vandervoort, N.; Christophe, T.; Mollat, P.; Lamers, M.; Auberval, M.; Hrvacic, B.; Ralic, J.; Oste, L.; van der Aar, E.; Brys, R.; Heckmann, B., Discovery of 2-[[2-Ethyl-6-[4-[2-(3-hydroxyazetidin-1-yl)-2-oxoethyl]piperazin-1-yl]-8-methylimidazo[1,2-a]pyridin-3-yl]methylamino]-4-(4-fluorophenyl)thiazole-5-carbonitrile (GLPG1690), a First-in-Class

Autotaxin Inhibitor Undergoing Clinical Evaluation for the Treatment of Idiopathic Pulmonary Fibrosis. *Journal of Medicinal Chemistry* **2017,** *60* (9), 3580-3590.
26. Ghumman, M.; Dhamecha, D.; Gonsalves, A.; Fortier, L.; Sorkhdini, P.; Zhou, Y.; Menon, J. U., Emerging drug delivery strategies for idiopathic pulmonary fibrosis treatment. *European Journal of Pharmaceutics and Biopharmaceutics* **2021,** *164*, 1-12.
27. Patra, J. K.; Das, G.; Fraceto, L. F.; Campos, E. V. R.; Rodriguez-Torres, M. d. P.; Acosta-Torres, L. S.; Diaz-Torres, L. A.; Grillo, R.; Swamy, M. K.; Sharma, S.; Habtemariam, S.; Shin, H.-S., Nano based drug delivery systems: recent developments and future prospects. *Journal of Nanobiotechnology* **2018,** *16* (1), 71.
28. Pramanik, S.; Mohanto, S.; Manne, R.; Rajendran, R. R.; Deepak, A.; Edapully, S. J.; Patil, T.; Katari, O., Nanoparticle-Based Drug Delivery System: The Magic Bullet for the Treatment of Chronic Pulmonary Diseases. *Molecular Pharmaceutics* **2021,** *18* (10), 3671-3718.
29. Qiao, H.; Liu, W.; Gu, H.; Wang, D.; Wang, Y., The Transport and Deposition of Nanoparticles in Respiratory System by Inhalation. *Journal of Nanomaterials* **2015,** *2015*, 394507.
30. Menon, J. U.; Ravikumar, P.; Pise, A.; Gyawali, D.; Hsia, C. C. W.; Nguyen, K. T., Polymeric nanoparticles for pulmonary protein and DNA delivery. *Acta Biomaterialia* **2014,** *10* (6), 2643-2652.
31. Conte, G.; Costabile, G.; Baldassi, D.; Rondelli, V.; Bassi, R.; Colombo, D.; Linardos, G.; Fiscarelli, E. V.; Sorrentino, R.; Miro, A.; Quaglia, F.; Brocca, P.; d'Angelo, I.; Merkel, O. M.; Ungaro, F., Hybrid Lipid/Polymer Nanoparticles to Tackle the Cystic Fibrosis Mucus Barrier in siRNA Delivery to the Lungs: Does PEGylation Make the Difference? *ACS Applied Materials & Interfaces* **2022,** *14* (6), 7565-7578.
32. Trivedi, R.; Redente, E. F.; Thakur, A.; Riches, D. W. H.; Kompella, U. B., Local delivery of biodegradable pirfenidone nanoparticles ameliorates bleomycin-induced pulmonary fibrosis in mice. *Nanotechnology* **2012,** *23* (50), 505101.
33. Boegh, M.; Nielsen, H. M., Mucus as a Barrier to Drug Delivery – Understanding and Mimicking the Barrier Properties. *Basic & Clinical Pharmacology & Toxicology* **2015,** *116* (3), 179-186.
34. Olmsted, S. S.; Padgett, J. L.; Yudin, A. I.; Whaley, K. J.; Moench, T. R.; Cone, R. A., Diffusion of Macromolecules and Virus-Like Particles in Human Cervical Mucus. *Biophysical Journal* **2001,** *81* (4), 1930-1937.
35. Huckaby, J. T.; Lai, S. K., PEGylation for enhancing nanoparticle diffusion in mucus. *Advanced Drug Delivery Reviews* **2018,** *124*, 125-139.
36. Suk, J. S.; Xu, Q.; Kim, N.; Hanes, J.; Ensign, L. M., PEGylation as a strategy for improving nanoparticle-based drug and gene delivery. *Advanced Drug Delivery Reviews* **2016,** *99*, 28-51.
37. Tang, B. C.; Dawson, M.; Lai, S. K.; Wang, Y.-Y.; Suk, J. S.; Yang, M.; Zeitlin, P.; Boyle, M. P.; Fu, J.; Hanes, J., Biodegradable polymer nanoparticles that rapidly penetrate the human mucus barrier. *Proceedings of the National Academy of Sciences* **2009,** *106* (46), 19268-19273.
38. Suk, J. S.; Lai, S. K.; Wang, Y.-Y.; Ensign, L. M.; Zeitlin, P. L.; Boyle, M. P.; Hanes, J., The penetration of fresh undiluted sputum expectorated by cystic fibrosis patients by non-adhesive polymer nanoparticles. *Biomaterials* **2009,** *30* (13), 2591-2597.

39. Yu, T.; Wang, Y.-Y.; Yang, M.; Schneider, C.; Zhong, W.; Pulicare, S.; Choi, W.-J.; Mert, O.; Fu, J.; Lai, S. K.; Hanes, J., Biodegradable mucus-penetrating nanoparticles composed of diblock copolymers of polyethylene glycol and poly(lactic-co-glycolic acid). *Drug Delivery and Translational Research* **2012,** *2* (2), 124-128.
40. Lai, S. K.; O'Hanlon, D. E.; Harrold, S.; Man, S. T.; Wang, Y.-Y.; Cone, R.; Hanes, J., Rapid transport of large polymeric nanoparticles in fresh undiluted human mucus. *Proceedings of the National Academy of Sciences* **2007,** *104* (5), 1482-1487.
41. Wang, Y. Y.; Lai Sk Fau - Suk, J. S.; Suk Js Fau - Pace, A.; Pace A Fau - Cone, R.; Cone R Fau - Hanes, J.; Hanes, J., Addressing the PEG mucoadhesivity paradox to engineer nanoparticles that "slip" through the human mucus barrier. (1521-3773 (Electronic)).
42. Wang, Y.-Y.; Lai, S. K.; Suk, J. S.; Pace, A.; Cone, R.; Hanes, J., Addressing the PEG Mucoadhesivity Paradox to Engineer Nanoparticles that “Slip” through the Human Mucus Barrier. *Angewandte Chemie International Edition* **2008,** *47* (50), 9726-9729.
43. Yazdani, S.; Bansal, R.; Prakash, J., Drug targeting to myofibroblasts: Implications for fibrosis and cancer. (1872-8294 (Electronic)).
44. Acharya, P. S.; Zukas A Fau - Chandan, V.; Chandan V Fau - Katzenstein, A.-L. A.; Katzenstein Al Fau - Puré, E.; Puré, E., Fibroblast activation protein: a serine protease expressed at the remodeling interface in idiopathic pulmonary fibrosis. (0046-8177 (Print)).
45. Hettiarachchi, S. U.; Li, Y.-H.; Roy, J.; Zhang, F.; Puchulu-Campanella, E.; Lindeman, S. D.; Srinivasarao, M.; Tsoyi, K.; Liang, X.; Ayaub, E. A.; Nickerson-Nutter, C.; Rosas, I. O.; Low, P. S., Targeted inhibition of PI3 kinase/mTOR specifically in fibrotic lung fibroblasts suppresses pulmonary fibrosis in experimental models. *Science Translational Medicine* **2020,** *12* (567), eaay3724.
46. Yang, P.; Fang, Q.; Fu, Z.; Li, J.; Lai, Y.; Chen, X.; Xu, X.; Peng, X.; Hu, K.; Nie, X.; Liu, S.; Zhang, J.; Li, J.; Shen, C.; Gu, Y.; Liu, J.; Chen, J.; Zhong, N.; Wang, X.; Luo, Q.; Su, J., Comprehensive Analysis of Fibroblast Activation Protein (FAP) Expression in Interstitial Lung Diseases (ILDs). LID - 10.1164/rccm.202110-2414OC [doi]. (1535-4970 (Electronic)).
47. Sundarakrishnan, A.; Chen, Y.; Black, L. D.; Aldridge, B. B.; Kaplan, D. L., Engineered cell and tissue models of pulmonary fibrosis. (1872-8294 (Electronic)).
48. Pezzulo, A. A.; Starner, T. D.; Scheetz, T. E.; Traver, G. L.; Tilley, A. E.; Harvey, B.-G.; Crystal, R. G.; McCray, P. B.; Zabner, J., The air-liquid interface and use of primary cell cultures are important to recapitulate the transcriptional profile of in vivo airway epithelia. *American Journal of Physiology-Lung Cellular and Molecular Physiology* **2010,** *300* (1), L25-L31.
49. Prasad, S.; Hogaboam, C. M.; Jarai, G., Deficient repair response of IPF fibroblasts in a co-culture model of epithelial injury and repair. *Fibrogenesis & Tissue Repair* **2014,** *7* (1), 7.
50. Yu, W.; Fang, X.; Ewald, A.; Wong, K.; Hunt, C. A.; Werb, Z.; Matthay, M. A.; Mostov, K., Formation of Cysts by Alveolar Type II Cells in Three-dimensional Culture Reveals a Novel Mechanism for Epithelial Morphogenesis. *Molecular Biology of the Cell* **2007,** *18* (5), 1693-1700.
51. Halwani, R.; Al-Muhsen, S.; Al-Jahdali, H.; Hamid, Q., Role of Transforming Growth Factor–β in Airway Remodeling in Asthma. *American Journal of Respiratory Cell and Molecular Biology* **2011,** *44* (2), 127-133.
52. Schöffski, P.; Adkins, D.; Blay, J. Y.; Gil, T.; Elias, A. D.; Rutkowski, P.; Pennock, G. K.; Youssoufian, H.; Gelderblom, H.; Willey, R.; Grebennik, D. O., An open-label, phase 2

study evaluating the efficacy and safety of the anti-IGF-1R antibody cixutumumab in patients with previously treated advanced or metastatic soft-tissue sarcoma or Ewing family of tumours. *European Journal of Cancer* **2013,** *49* (15), 3219-3228.
53. Huang, X.; Wang, X.; Xie, X.; Zeng, S.; Li, Z.; Xu, X.; Yang, H.; Qiu, F.; Lin, J.; Diao, Y., Kallistatin protects against bleomycin-induced idiopathic pulmonary fibrosis by inhibiting angiogenesis and inflammation. (1943-8141 (Print)).
54. Grinnell, F., Fibroblast biology in three-dimensional collagen matrices. (0962-8924 (Print)).
55. Kadler, K. E.; Hill, A.; Canty-Laird, E. G., Collagen fibrillogenesis: fibronectin, integrins, and minor collagens as organizers and nucleators. *Current Opinion in Cell Biology* **2008,** *20* (5), 495-501.
56. Arora, P. D.; Narani N Fau - McCulloch, C. A.; McCulloch, C. A., The compliance of collagen gels regulates transforming growth factor-beta induction of alpha-smooth muscle actin in fibroblasts. (0002-9440 (Print)).
57. Travis, J. A.; Hughes, M. G.; Wong, J. M.; Wagner, W. D.; Geary, R. L., Hyaluronan Enhances Contraction of Collagen by Smooth Muscle Cells and Adventitial Fibroblasts. *Circulation Research* **2001,** *88* (1), 77-83.
58. Seraglio, S. K. T.; Silva, B.; Bergamo, G.; Brugnerotto, P.; Gonzaga, L. V.; Fett, R.; Costa, A. C. O., An overview of physicochemical characteristics and health-promoting properties of honeydew honey. *Food Research International* **2019,** *119*, 44-66.
59. Menon, J. U.; Ravikumar, P.; Pise, A.; Gyawali, D.; Hsia, C. C.; Nguyen, K. T., Polymeric nanoparticles for pulmonary protein and DNA delivery. (1878-7568 (Electronic)).
60. Casciaro, B.; d'Angelo, I.; Zhang, X.; Loffredo, M. R.; Conte, G.; Cappiello, F.; Quaglia, F.; Di, Y.-P. P.; Ungaro, F.; Mangoni, M. L., Poly(lactide-co-glycolide) Nanoparticles for Prolonged Therapeutic Efficacy of Esculentin-1a-Derived Antimicrobial Peptides against Pseudomonas aeruginosa Lung Infection: in Vitro and in Vivo Studies. *Biomacromolecules* **2019,** *20* (5), 1876-1888.
61. Alsharabasy, A. M.; Pandit, A., Protocol for in vitro skin fibrosis model to screen the biological effects of antifibrotic compounds. *STAR Protocols* **2021,** *2* (1), 100387.
62. Mecozzi, L.; Mambrini, M.; Ruscitti, F.; Ferrini, E.; Ciccimarra, R.; Ravanetti, F.; Sverzellati, N.; Silva, M.; Ruffini, L.; Belenkov, S.; Civelli, M.; Villetti, G.; Stellari, F. F., In-vivo lung fibrosis staging in a bleomycin-mouse model: a new micro-CT guided densitometric approach. *Scientific Reports* **2020,** *10* (1), 18735.
63. Ravanetti, F.; Ragionieri, L.; Ciccimarra, R.; Ruscitti, F.; Pompilio, D.; Gazza, F.; Villetti, G.; Cacchioli, A.; Stellari, F. F., Modeling pulmonary fibrosis through bleomycin delivered by osmotic minipump: a new histomorphometric method of evaluation. *American Journal of Physiology-Lung Cellular and Molecular Physiology* **2019,** *318* (2), L376-L385.
64. Pereira, E.; Cerruti, R.; Fernandes, E.; icart, L.; Saez, V.; Pinto, J.; Ramón, J.; Oliveira, G.; Souza Jr, F., Influence of PLGA and PLGA-PEG on the dissolution profile of oxaliplatin. *Polímeros* **2016,** *26*.
65. García-Díaz, M.; Birch, D.; Wan, F.; Nielsen, H. M., The role of mucus as an invisible cloak to transepithelial drug delivery by nanoparticles. (1872-8294 (Electronic)).
66. Duncan, G. A.; Jung, J.; Hanes, J.; Suk, J. S., The Mucus Barrier to Inhaled Gene Therapy. (1525-0024 (Electronic)).
67. Wine, J. J.; Hansson, G. C.; König, P.; Joo, N. S.; Ermund, A.; Pieper, M., Progress in understanding mucus abnormalities in cystic fibrosis airways. (1873-5010 (Electronic)).
68. Turcios, N. L., Cystic Fibrosis Lung Disease: An Overview. (1943-3654 (Electronic)).

69. Lai, S. K.; Wang Yy Fau - Hanes, J.; Hanes, J., Mucus-penetrating nanoparticles for drug and gene delivery to mucosal tissues. (1872-8294 (Electronic)).
70. McKleroy, W.; Lee, T.-H.; Atabai, K., Always cleave up your mess: targeting collagen degradation to treat tissue fibrosis. *American Journal of Physiology-Lung Cellular and Molecular Physiology* **2013,** *304* (11), L709-L721.

Biographical Information

I was born and brought up in Chennai, India. After high school, I pursued my bachelor's degree in Nanotechnology at SRM Institute of Science and Technology. During my bachelor's degree, I worked on nanoparticles based for medical cancer imaging under the guidance of Dr. K. D. Nisha. Post completing my bachelor's degree, I joined UTA in 2017 as a masters student, I joined Dr. Kytai Nguyen's lab as a research volunteer from day 1 and was given an opportunity to pursue B.S to Ph.D. from 2018 under her guidance, where I worked on several projects with nanoparticles as targeted drug delivery systems. As a doctoral student, I received several awards such as the Dr. Franklyn Alexander scholarship for outstanding student and academic excellence, a STEM fellowship for graduate teaching and research assistant. I mentored and trained 4 senior design student projects, to help them develop medical devices which are in the process of patents. I have been active in the academic affairs representing the bioengineering department for high school lab tours. I have 5 research papers published, several in preparation, 6 conference proceedings and two patent applications. Following my Ph.D., I plan to continue my academic career in the field of nanotechnology based drug delivery.

Peer-reviewed Publications (*Denotes Co-first Author)

- **R. Harish***, K.D. Nisha, S. Prabakaran, B. Sridevi, S. Harish, M. Navaneethan, S. Ponnusamy, Y. Hayakawa, C. Vinniee, M.R. Ganesh; Cytotoxicity assessment of chitosan coated CdS nanoparticles for bio-imaging applications. Applied Surface Science, Volume 499, 2020.

- Yaman S, **Ramachandramoorthy H***, Oter G, Zhukova D, Nguyen T, Sabnani MK, Weidanz JA and Nguyen KT; Melanoma Peptide MHC Specific TCR Expressing T-Cell Membrane Camouflaged PLGA Nanoparticles for Treatment of Melanoma Skin Cancer. frontiers in bioengineering and biotechnology , 8:943, 2020.

- Iyer R, **Ramachandramoorthy H***, Nguyen T, Xu C, Fu H, Kotadia T, Chen B, Hong Y, Saha D, Nguyen KT; Lung Cancer Targeted Chemoradiotherapy via Dual-Stimuli Responsive Biodegradable Core-Shell Nanoparticles. Pharmaceutics, 14(8):1525, 2022.

- Yaman S, Chintapula U, Rodriguez E, **Ramachandramoorthy H**, Nguyen KT. Cell-mediated and cell membrane-coated nanoparticles for drug delivery and cancer therapy. Cancer Drug Resist, 3:879-911, 2020.

- Qhobosheane R, **Ramachandramoorthy H**, Bhattarai B, Livingston K, Nguyen T, Nguyen KT, Shen W; An on-Chip Microfluidic Device for Production of Liposomes. Biodevices, 2020.

Patent applications

- Kytai Truong Nguyen, Alan Nguyen, **Harish Ramachandramoorthy**, Daniel To, Dylan Yu. Automated gas control hypoxic chamber for monitoring oxygen concentration. PCT/US20210348110A1. Publication 2021.

- Kytai Truong Nguyen, **Harish Ramachandramoorthy**, Serkan Yaman, Manoj Sabnani, Jon A Weidanz. Double Sided Chimeric Antigen Receptor (CAR) Engineered Cell Membrane Based Drug Delivery Systems. PCT/US2022/027883. Publication 2022.